Transportation Research Part C 144 (2022) 103860

Contents lists available at ScienceDirect

Transportation Research Part C

journal homepage: www.elsevier.com/locate/trc

Unified network tRaffic management frAmework for fully conNected and electric vehicles energy cOnsumption optimization (URANO)

Roberta Di Pace [a,*], Chiara Fiori [a], Facundo Storani [a], Stefano de Luca [a], Carlo Liberto [b], Gaetano Valenti [b]

[a] Laboratory of Transportation Systems Engineering and Sustainable Mobility (ISTMoS) Department of Civil Engineering, University of Salerno, via Giovanni Paolo II, 132 84084 Fisciano, SA, Italy

[b] Laboratory of Systems and Technologies for Sustainable Mobility & Electric Energy Storage, ENEA, via Anguillarese 301, 00123 Rome, Italy

ARTICLE INFO

Keywords:
Traffic control
Multi-objective
Electric powertrain
Energy consumption/recovery
Calibration

ABSTRACT

Cooperative control in the presence of connected and automated vehicles has attracted substantial attention due to its pronounced benefits on the network compared with human-driven vehicles. They make possible a significant reduction of travel time/waiting time, energy consumption and emissions. In this context of new emerging technologies, traffic lights are still recognized as one of the most effective strategies in terms of energy and environmental benefits, which can be further improved by considering the integration with greener powertrains. The paper proposes a cooperative network traffic management framework for Electric Vehicles (EVs) based on a multi-objective optimization aimed at minimizing the total time spent (TTS) and energy consumption (EC) of EVs. Such framework is composed of i) a traffic control model that incorporates traffic lights design, ii) a traffic flow model to estimate TTS as a network performance indicator, and iii) an EVs model to estimate EC at the intersections. The EC function has been derived from a VT-CPEM model to simulate consumptions and thoroughly calibrated based on real-world individual trajectories. The optimization framework was implemented on a nine-node network and the results of the multi-criteria optimization (aiming at minimizing the TTS and EC of EV) are compared with results of the benchmark mono - criterion optimization (aiming at minimizing the TTS) and the mono-criterion optimization combined with the speed advisory (GLOSA; Green Light Optimized Speed Advisory). All the proposed analyses were carried out for different powertrain vehicle categories; ICEVs, and EVs.

1. Introduction and motivation

If the future of personal transportation will be connected and electric, it will continue to be based on cars and physical infrastructure. In this framework, the challenge of the next years will be to develop strategies that harmonize drivers, technologies, and infrastructures to maximize the level of service and energy efficiency (i.e., consumption and, emissions) of fully connected transportation system.

The literature is rich in contributions that attempt to address such issues at different scales. Indeed, great attention has been paid to

* Corresponding author.

https://doi.org/10.1016/j.trc.2022.103860
Received 18 September 2021; Received in revised form 11 July 2022; Accepted 9 August 2022
Available online 18 September 2022

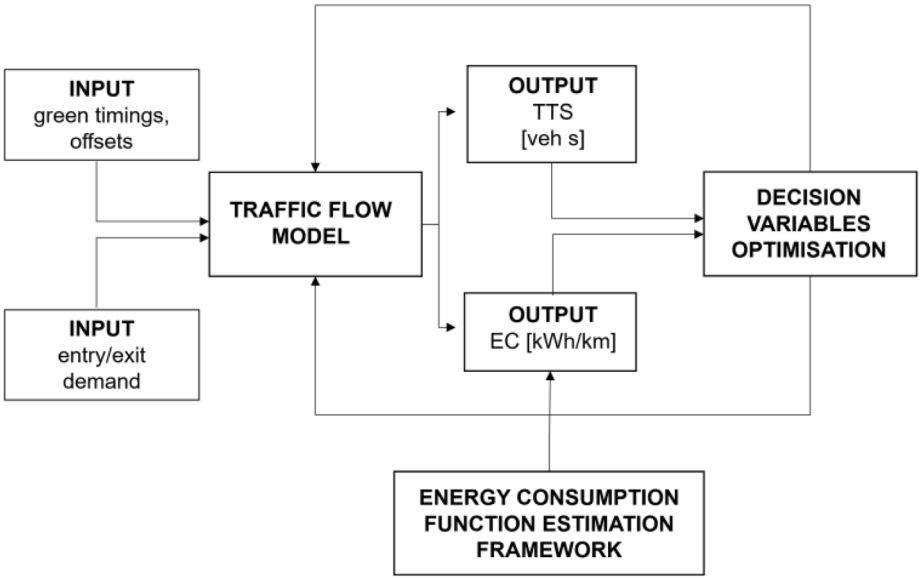

Fig. 1. Overview of the URANO whole framework.

non-urban and urban levels and, in particular, to isolated (e.g., single, Cantarella et al., 2015) and interacting junctions (e.g., artery, network, Girianna and Benekohal, 2004) in the second case.

To date, several studies have shown that enhanced strategies based on connected and automated control and, in particular, speed advisory, can significantly reduce network performance (e.g., total time spent, travel time, delay time, etc.) compared to networks with human-driven vehicles (Fajardo et al., 2011; Liebner et al., 2013; Feng et al., 2015). Moreover, these strategies also affect energy consumption and emissions; for this reason, proper optimization of traffic lights at intersections may lead to significant energy and environmental benefits. Specifically, with proper designs of the above-mentioned strategies combined with greener powertrains, it is possible to achieve different objectives such as travel time savings and reduced energy consumption and emissions.

The expected benefits depend on technological contexts (i.e., connectivity, automation, and powertrain) and the controllable variables (Levin and Boyles, 2016a; Zhou et al., 2017; Zhu and Ukkusuri, 2017, 2018). For various technological contexts, the different levels/types of connectivity, automation, and powertrains may significantly affect the impact of the adopted control strategies and, thus, the potential achievable benefits.

The main challenge is to properly design the control strategies in the presence of connected and electric vehicles (i.e., CVs, EVs). However, the design of control strategies in the presence of CVs can rely on existing research findings (Stevanovic et al., 2009; Priemer and Friedrich, 2009; He et al., 2015; Goodall et al., 2013; Lee et al., 2013; Feng et al., 2015, 2016; Al Islam and Hajbabaie, 2017; Beak et al., 2017;Wang et al., 2015; Wang et al., 2016; Han et al., 2021), by contrast, the design in the presence of EVs remains a challenging task.

Indeed, EVs are characterized by higher onboard efficiency and a consequent reduction in energy consumption. On the other hand, in contrast to internal combustion engine vehicles (ICEVs), the minimization of total time spent (TTS[1]) does not guarantee minimum energy consumption for EVs. Indeed, EVs are characterized by a direct relationship between congestion and the energy consumption underlying a higher energy consumption with an increased average traffic speed (Fiori et al., 2019).

For this reason, specific strategies coherent with the EVs consumption function are needed.

To date, each of the above-mentioned issues has been studied in the literature. Several studies have investigated vehicles speed optimization strategies only through eco-driving strategies, such as variable speed algorithms for arterial traffic commonly known as the Green Light Optimized Speed Advisory (GLOSA) system (Katsaros et al., 2011) or through individual dynamic speed advice aimed at optimizing the speed profiles (Asadi and Vahidi, 2010; Bandeira et al., 2018; Kamalanathsharma et al., 2015; De Nunzio et al., 2016). Other studies have focused on the development of fuel economic control strategies for a single - vehicle without considering the impact on other vehicles (HomChaudhuri et al., 2017; Zhou et al., 2017; Ma et al., 2017) while few studies have attempted to optimize the fuel consumption of platoons (Zhao et al., 2015).

However, very few studies have investigated the use of traffic light signals for fuel consumption and emission reduction (Stevanovic et al., 2009; Zhao et al., 2021; Zegeye et al., 2009; Zegeye et al., 2013).

In particular, Stevanovic et al. (2009) proposed an integrated tool for offline traffic signal timing optimization combining fuel consumption and emission reduction, while Zegeye et al. (2009) designed a model predictive control (MPC) strategy focusing on online

[1] The TTS is defined as the sum of the number of vehicles on each link for each time step, for the whole simulation interval. Further details are provided in the following in the Section 2.1.3.

Fig. 2. Scheme of the control zone and V-to-infrastructure communication.[1] [1]The sum of feedback and vehicle actuation delays is assumed to be less than 1 s and hence can be neglected in the control formulation when we choose a discrete time step size of 1 s (see Liu et al., 2022).

control of both the total travel time and total emissions. Zegeye et al. (2013) proposed a framework combining macroscopic traffic flow models and microscopic emission and fuel consumption models for freeway traffic networks. At the urban level, Zhu et al. (2013) adopted a similar approach aimed at minimizing delays and emissions.

Finally, very few studies have considered the presence of EVs; for instance, Li and Ban (2018) developed a framework suitable for the coordination of multiple signals in the presence of connected and automated vehicles (CAVs), and the considered objective functions were the energy consumption and travel time. In general, studies on this topic adopt models with some limitations for the evaluation of EV energy consumption. For example, Luo et al. aimed to develop a novel optimal speed advisory board strategy for successive intersections of hybrid vehicles (Luo et al., 2017). For the energy consumption model, they adopted fuel/energy consumption maps that can exclusively be generated by testing a vehicle on an engine or chassis dynamometer. Therefore, there are critical limitations on the adaptability of these models, as reported by some studies (Fiori et al., 2018; Park et al., 2013).

In this context, a multi-objective optimization framework should be pursued, including traffic control, traffic flow, and EV energy consumption models. This study proposes a multi-objective optimization framework that aims at minimizing the TTS and energy consumption (EC) of EVs in a fully connected transportation system. To meet this aim three models are implemented:

1. a traffic control model aiming at a design that incorporates traffic lights
2. a traffic flow model for estimating TTS as a network performance indicator
3. an EVs model for estimating EC at the intersections.

In more detail, the framework is a Unified Network traffic Management framework based on the cooperAtive OptimizatioN of Electric Vehicles Energy COnsumption (i.e., URANO). This is illustrated in Fig. 1.

The optimization framework has been implemented on a nine-node network where once the vehicles approach the control zone[2] they are assumed to be fully connected, and information are exchanged between each vehicle and the traffic signal controller (see Fig. 2).

The main contribution of the study is twofold:

1. The multi-objective optimization including EV energy consumption optimization has been specified and applied.
2. All analyses proposed above are carried out for different powertrain vehicle categories, ICEVs, and EVs. In this study, a link-based macroscopic energy consumption function for EVs was derived from microscopic data. The adopted function was derived based on the VT-CPEM model to simulate consumption at a signalized intersection. The model was thoroughly calibrated based on real-

[2] The control zone is identified as the region centered on each signalized intersection; vehicles within the control zone are connected with the infrastructure.

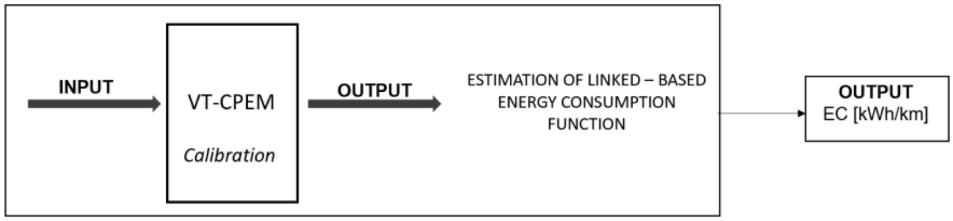

Fig. 3. Aggregate overview of the EV energy consumption function estimation framework.

world individual trajectories at signalized intersections. In more detail, the model requires as inputs the instantaneous speed, grade, payload on-board and the vehicle characteristics, and produces as output the energy consumption (EC) [kWh/km] by the vehicle for a specific drive cycle, the instantaneous power consumed [kW], and the State Of Charge (SOC) of the electric battery [%] at the end of the simulation. Finally, the model estimates the energy consumption. The adoption of the VT-CPEM model (Fiori et al., 2016), makes it possible to overcome the previously mentioned limitations, such as the use of efficiency maps, and to quantify the energy while braking, that is, the so-called energy efficiency recovery as a function of the deceleration levels. An aggregate overview of the model is shown in the following Fig. 3.

Furthermore, a comparison between the proposed multi-objective control strategy and the mixed (combining traffic control and speed optimization) strategy is performed. Finally, considering that CVs will increase but in the short term, traffic flow conditions are expected to be mixed, considering the relevant role of human-driven vehicles (Levin and Boyles, 2016a, 2016b), different penetration rates of CVs are analyzed.

The remainder of the paper is organized as follows: Section 2 discusses the theoretical framework, with Section 2.1 concerning multi-objective traffic lights optimization and Section 2.2 discusses the energy consumption of EVs and the description of all steps necessary to derive the specific link-based macroscopic energy consumption function for EVs. Section 3 details the experiment setup and the numerical results, and Section 4 summarizes the conclusions and future works to be undertaken.

2. Theoretical framework

This section aims at describing the three models composing the proposed framework and, in particular:

1. a traffic control model aiming at a design that incorporates traffic lights (see Section 2.1);
2. a traffic flow model for estimating TTS as a network performance indicator (see Appendix A[3]);
3. an EVs model for estimating EC at the intersections (see Section 2.2).

2.1. Multi-objective network traffic lights

2.1.1. Problem statement

In this section, the details of the multi-objective traffic control problem are discussed. First, it must be specified that the adopted approaches refer to interacting intersections (Robertson, 1979), in which the arrival flows at downstream intersections depend on the arrival flows at the same intersection in the previous time interval, on the arrival flows upstream on the same interval, while the delays at downstream intersections depend on the flows entering upstream. It is widely known that the main decision variables of traffic light control are the stage durations, sequences, and cycle length. For interacting intersections, the offsets that define when the signal settings of each intersection start for a given clock reference must be considered. However, the most frequently considered variables are the stage durations and offsets. Furthermore, concerning the optimisation of stage sequences, it is demonstrated that it can be neglected when the number of stages is strictly less than four. In more detail, Memoli et al. (2017) discussed the problem at the network level by introducing the equivalence class definition depending on the number of stages. They also demonstrated that the optimisation of stage sequences has a significant effect when the number of stages is higher than three. In this paper, the considered decision variables are the stage durations and the offsets. The settings of the numerical application are consistent with the accuracy degree. To solve the problem, the simultaneous (single layer) or sequential method can be applied; in the first method, the stage durations and offsetGs are optimized together, whereas, in the second method, the optimization procedure is run in two successive steps. In this study, simultaneous optimization was applied. In general, two main applications are identified for objective functions: the first for mono-criterion optimization, and the second for multi-objective optimization. As mentioned in the introduction, the focus of this study is on the multi-objective problem combining the TTS and EC. To this end, the traffic flow is modelled through a hybrid model based on the combination of the Cellular Automata (CA; Nagel and Schreckenberg, 1992) and Cell Transmission Model (CTM; Daganzo, 1994), which is the H-CA &CTM properly designed to support the analysis of the control strategies in the presence of CAVs. For completeness,

[3] A detailed description of the model is discussed in Storani et al. (2021, 2022a, 2022b).

to support the readers, the general overview of the considered traffic flow model is provided in Appendix A.

2.1.2. Variable's definition

Let the intersection network be represented by an undirected graph with a node for each intersection and an edge for each pair of adjacent intersections (the actual traffic directions are irrelevant), with m nodes as the number of intersections. Assuming that the green scheduling is described by the stage composition and their sequence, let.

$c > 0$ be the cycle length, common to all intersections, assumed known or as an optimization variable, often constrained in a given range.

For each intersection (not explicitly indicated) let.

$t_j \in [0, c]$ be the length of stage j as an optimization variable; if no minimum length constraint is introduced, the optimal length of a (optional) stage may be zero, meaning that this stage is not in the optimal solution;

$t_{ar} \in [0, c]$ be the so-called all-red period at the end of each stage to allow for the safe clearance of the intersection, assumed known (and constant for simplicity's sake);

$l_k \in [0, c]$ be the lost time for approach k, assumed known[4];

$g_k = \sum_j \hat{I}_{kj} t_j - t_{ar} - l_k \in [0, c]$[5] be the effective green for approach k needed for computing the total time spent through a traffic flow model.

$q_k > 0$ be the arrival flow for approach k, assumed known;

$s_k > 0$ be the saturation flow for approach k, assumed known.

Apart from non-negativity of optimization variables, a constraint[6] needs to be introduced for each intersection to guarantee consistency among the stage lengths and the cycle length:

$$\sum_j t_j = c$$

Moreover, for each intersection i let.

$\phi \in [0, c[$ be the node offset between the start of a reference stage of intersection i and the start of the reference stage of the first intersection used as a reference for clock, $\phi_1 = 0$, thus the number of the independent node offsets is $m - 1$.

For each pair of (adjacent) intersections (i, h) in the network, let.

$\phi_{ih} = \phi_h - \phi_i = -\phi_{hi}$ be the link offset[7] between intersections i and h, needed for computing total times spent through a traffic flow model.

2.1.3. Model formulation and solution

This section discusses the adopted criteria for the formulation of the optimization problem. In particular, the two criteria identified as objective functions are the total time spent (TTS) and the total energy consumption (EC) considering all the vehicles with an electric powertrain.

The Total Time Spent is calculated as the sum of the observed number of vehicles on all the links of the network, during the simulation horizon, multiplied by the length of each time step. However, since the simulation starts with an empty network, a first warm-up period was considered in which the indicator is not calculated. Then, the simulation continues with a simulation horizon of 3600 s, with a time step of 1 s. Furthermore, the considered step size equal to 1 s is higher than the interval necessary for the feedback's exchanges and the vehicles' reaction. Furthermore, still concerning the TTS, it must be clarified that in the case of traffic lights optimization, the TD is considered an objective function to minimize to increase the performance of intersections. In this case, the proposed procedure also aims to optimize energy consumption. Given that the energy consumption depends on vehicles' speed, the latter may be regarded as a proxy variable of energy consumption. For this reason, we considered the TTS in the proposed modelling

[4] It is composed of two terms: the start-up lost time which occurs every time a queue of vehicles starts moving on a green signal and the clearance lost time that is a lost time associated with stopping the queue at the end of the green signal and it occurs each time a flow of vehicles is stopped. This is defined as the time interval between the last vehicle's front wheels crossing the stop line and the initiation of the green signal for the next stage. The clearance time is considered to eliminate conflictions between incompatible vehicle movements within an intersection area (see Roess et al., 2004).The start-up lost time may be eliminated in a scenario of full CVs penetration (Ma et al., 2022), thus allowing for more vehicles passing the intersection. However, it is necessary to consider that, in the proposed study, the cycle lengths are not part of the decision variables. As a result, even though the duration of the stages depends on the presence of CVs, they are constrained to the cycles' lengths.

[5] Non-negative effective green is usually guaranteed by the non-negative stage length, but for a very short cycle length with regard to the values of all-red period length and lost times, say the cycle length is less than $\sum_j MAXk(\delta_{kj} l_k + t_{ar})c$, this condition is never met in practical applications.

[6] Other constraints are sometimes used to guarantee the minimum value of the effective green $g_k g_{min} \forall_k$ and that the capacity factor is >1 (or any other value assumed as a threshold) $\left(\frac{s_k \bullet g_k}{c \bullet q_k}\right) \geq 1$ Such a constraint may be added only after having checked that the maximum intersection capacity factor for each approach k in the intersection i is >1, otherwise, a solution may not exist whatever the objective function is; concerning the minimum value of the effective green $g_k g_{min} \forall_k$ this has been not included considering the presence of CVs.

[7] If the network contains $k > 0$ independent loops, the number of independent link offsets is equal to m-k, thus it is better to use the $m - 1$ independent node offsets as optimization variables to avoid a useless increase of the number of variables and of constraints. On the other hand, if the network is loop-less, all the $m - 1$ link offsets are independent, as many as the independent node offsets, and might be used as optimization variables instead of the independent node offsets; arterials are a special case of such kind of networks.

framework. However, the TTS may be described through two components: a running travel time (the ratio between links length and speed) and waiting (delay) travel time. The running travel time is directly related to the energy consumption, thus, to analyze the consistency between the TTS and the consumption estimation, the speed (input variable of the consumption function) was computed for all vehicles in each link.

Let:

- t be the time step
- T_1 be the initial warm-up period
- T be the Simulation horizon
- l be the link belonging to the set of links L of the network
- n_l the number of vehicles in link l
- Δt be the length of the time step

Then, the TTS is obtained as:

$$TTS = J_{TTS} = \sum_{t=T_1}^{T_1+T} \sum_{l \in L} n_l \cdot \Delta t \tag{1}$$

The energy consumption (EC) is calculated considering all the vehicles with an electric powertrain (100 % of EVs rate). Its value is obtained from the sum of the energy consumption of all vehicles at each link, from the time taken to travel such link.

In particular, let:

- t be the time step
- T_1 be the initial warm-up period
- T be the Simulation horizon
- l be the link belonging to the set of links L of the network

i be the vehicle index.

- ΔT_l^i be the delta time for the vehicle i to travel (to enter and exit) the link l
- Δx_l be the length of the link l [m]
- $\bar{v}_l^i$ be the mean speed of vehicle i on link l
- $f\left(\bar{v}_l^i\right)$ be the energy consumption of each vehicle in kWh/km, obtained from its speed in km/h.
- EC_l^i be the mean energy consumption of the vehicles at each link, for each time step
- EC_{N,T_1-T} be the energy consumption of the vehicles for the entire network N, between the initial warmg-up period T_1 and the Simulation horizon T

The delta time for the vehicle i to travel (to enter and exit) the link l is calculated as:

$$\Delta T_l^i = t_l^{i,exit} - t_l^{i,enter} \text{ if } t_l^{i,enter} \geq T_1 \tag{2}$$

Then, the mean speed of vehicle i on link l is obtained as:

$$\bar{v}_l^i = \frac{\Delta x_l}{\Delta T_l^i} \left[\frac{m}{s}\right] \tag{3}$$

The energy consumption of vehicle i on link l is calculated as:

$$EC_l^i = f\left(\bar{v}_l^i \cdot 3.6\right) \cdot \frac{\Delta x_l}{1000} [kWh] \tag{4}$$

and the specific energy consumption is described in more detail in Section 2.2.[8]

Lastly, the Energy Consumption (EC) is calculated as:

$$EC_{N,T_1-T} = J_{EC} = \sum_{l \in L} \sum_{i \in l} EC_l^i \tag{5}$$

Since the problem is a multi-objective optimization, a single point of the solution set that minimizes all the objectives simultaneously generally does not exist. Therefore, to find and choose a suitable solution, it is necessary to calculate a weighted sum of the transformed objective functions, aiming to minimize the distance to the Utopia Point, that is, the point which has the minimum of each of the objective functions as coordinates.

[8] In the numerical applications also the ICEV energy consumption function has been considered (see Fiori et al., 2019).

Each objective function is transformed using the *upper-lower-bound approach* (Koski, 1981; Koski and Silvennoinen, 1987; Rao and Freiheit, 1991; Yang et al., 1994) therefore let:

- $J_o(\boldsymbol{x})$ be the objective function o, valuated at variables $\boldsymbol{x}$;
- $J_o^{\min Pareto}$ be the minimum value of the objective function o, coordinate of the utopia point;
- $J_o^{\max Pareto} = \max_{1\le j\le k}\left(J_o\left(\boldsymbol{x}_j^*\right)\right)$ be the Pareto maximum of the objective function o, with $\boldsymbol{x}_j^*$ being the point that minimizes the j-th objective function (such that is a vertex of the Pareto optimal set in the design space and $J_o\left(\boldsymbol{x}_j^*\right)$ is a vertex of the Pareto optimal set in the criterion space), coordinate of the nadir point;

The transformed objective function can be obtained as.

$$J_o^{trans} = \frac{J_o(\boldsymbol{x}) - J_o^{\min Pareto}}{J_o^{\max Pareto} - J_o^{\min Pareto}} \tag{6}$$

Then, the solution with the closest distance to the Nadir point was chosen, that is:

$$\min_{\boldsymbol{x}} U = \min_{\boldsymbol{x}} \sqrt{J_{TTS}^{trans}(\boldsymbol{x})^2 + J_{EC}^{trans}(\boldsymbol{x})^2} \tag{7}$$

Finally, the model has been run in terms of static approach (see TRANSYT; 1969) and in terms of solution algorithm, a meta-heuristic procedure has been adopted and in particular in this case, the Differential Evolution method (O'Hora et al., 2006; Price, 2013) was used.

There is no proof of convergence for DE, however, it has been shown to be effective on a large range of classic optimization problems. In a comparison by (Storn and Price, 1997) DE was more efficient than simulated annealing and genetic algorithms (Ali and Törn, 2004) found that DE was both more accurate and more efficient than controlled random search and another genetic algorithm. Lampinen and Storn (Lampinen and Storn, 2004) demonstrated that DE[9] was more accurate than several other optimization methods including four genetic algorithms (GA), simulated annealing (SA) and evolutionary programming.

In this research, DE was applied with the following parameter settings:

- Population size: variable depending on each scenario
- Combination probability: 0.90
- Scale factor F: $0.50 \cdot (1 + rand)$
- Maximum iterations: 1000

The population size is set equal to 5 times the number of variables, multiplied by the control horizon (Storn and Price, 1997). The control variables are the duration of the green light at each approach and the absolute (node) offset of the traffic light plans of each junction (minus one used as reference). *rand* is a random value generated with a uniform distribution between 0 and 1, giving, as a result, a *DE with random scale factor* with the aim to reduce the risk of stagnating at a local optimum (Das et al, 2005).

2.2. EV link-based energy consumption function

2.2.1. State of art and model overview

In particular, Zhang and Yao (2015) analyzed the EV eco-driving at signalized intersections using an EV data-driven model tested on the New European Driving Cycle (NEDC), which is no longer an accurate representation of average driving behavior. Indeed, on the 1st of September 2017 a new measure, the Worldwide harmonized Light-duty Test Procedure (WLTP) was introduced. This testing procedure has been developed under the supervision of the UNECE (United Nations Economic Commission for Europe), to provide uniform and more realistic test conditions worldwide (Pavlovic et al., 2016). Liu et al., (2019) in their work on eco-speed guidance for the mixed traffic of electric vehicles and internal combustion engine vehicles at an isolated signalized intersection, for EVs used data from Wu et al. (2015a) model based on a specific case scenario. Also, Wu et al. (2015b) in their study about the energy-optimal speed control for electric vehicles on signalized arterials used a data-driven model on a test vehicle that is not one of the commercially produced vehicles and this might bring biases the testing results which needed to be further verified using current commercially produced EVs. Furthermore, very few studies are available on the integration of EVs' with traffic control (Li et al., 2018) and on the combined analyzes of the EVs' consumption between traffic control decision variables optimization. Zhao et al., (2015) developed a traffic signal optimization incorporating different vehicle fuel consumption characteristics (including the EVs); the proposed multi-objective strategy aiming at the optimization of total energy consumption and traffic delay, focused only on isolated intersections. Other contributions in the current literature of EV are about the combined analysis of the driving behavior (energy-saving strategies; Luo et al., 2017) and traffic control. Furthermore, some specific considerations must be done regarding the energy consumption

[9] Different meta-heuristics have been compared in particular the DE has been compared to the SA and the GA in terms of effectiveness and efficiency. The results are not shown for sake of brevity.

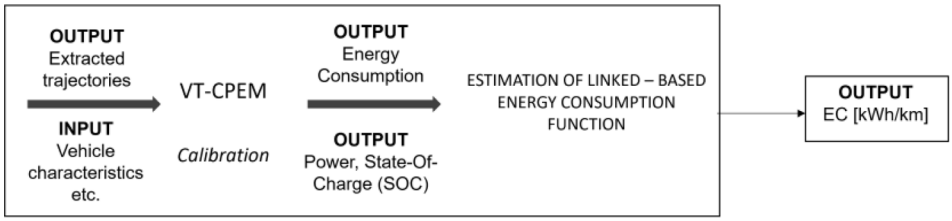

Fig. 4. An overview of the EV energy consumption function estimation framework.

function in the specific case of EV. Real-world simulation of fuel consumption of conventional vehicles is a well-known research area. The majority of these studies use models based on the efficiency map of the vehicle engine, either provided by the manufacturer or generated by testing the vehicle on a chassis dynamometer (Brooker et al., 2015; Kim et al., 2012; Lee et al., 2013; Newman et al., 2016; Wipke et al., 1999). A common drawback of simulation models available is that they critically depend upon the availability of efficiency maps, significantly varying by type of vehicle, yielding transferability issues and limited application flexibility. In addition, automakers, the only ones who could provide efficiency maps, are reluctant to share these maps because of obvious industry-related protection policies. To overcome this shortcoming, some models have been developed for conventional vehicles (Rakha et al., 2011). Specifically, Rakha et al., (2011) adopted a second-order polynomial to approximate the convexity of the fuel consumption function in the range of positive values, attaining a good compromise between model accuracy and applicability. The model was proved to predict well vehicle fuel consumption rates and CO2 emissions consistent with in-field measurements. Following a similar approach, (Fiori et al., 2016; Fiori et al., 2018; Fiori and Marzano, 2018, Fiori et al., 2020) generalized the above model to the powertrain of electric vehicles (EVs) and electric freight vehicles (EFVs), by developing the Virginia Tech Comprehensive Power-based EV Energy consumption Model (VT-CPEM) and the EFVs energy consumption model (EFVs-ECM), respectively, aimed at evaluating the vehicle energy consumption as a function of vehicle's speed profile and characteristics, independently of efficiency maps. Notably, these models were estimated and validated based on real data. Another interesting and unique feature is their capability to quantify the energy while braking, i.e., the so-called energy efficiency recovery, as a function of the deceleration levels.

This study adopts the VT-CPEM model (Fiori et al., 2016), which does not suffer from the previously mentioned limitations, such as the use of efficiency maps, re-calibrated on a specific dataset of real-world data including signalized intersection.

In particular, a specific energy consumption function has been derived based on the VT-CPEM model to simulate consumptions at signalized intersections. The model has been thoroughly calibrated based on real-world individual trajectories at signalized intersections. Furthermore, to support the trajectories extraction from a large dataset an innovative tool has been developed and integrated with the whole EC framework - Trajectories Extraction Tool for Traffic Control Systems Applications (TET-TCSA) (see Appendix B for additional details). To be more precise, the portion of vehicle trajectories in the proximity of signalized intersections have been extracted and used to feed a microscopic energy consumption model of electric vehicles - VT-CPEM, (Fiori et al., 2016). By running the model in a quasi-Monte Carlo framework, an energy consumption function is estimated.

In the following the model details are shown, describing: *i)* the vehicle simulator for EVs, *(ii)* the trajectory extraction tool, *(iii)* the VT-CPEM calibration with reference to the signalized interacting intersections real data, and *(iv)* the estimation of the link-based energy consumption. For the sake of brevity, the details of the vehicle simulator for EVs and the estimation of the link-based energy consumption are provided in the following sections whereas the detail of the trajectory extraction tool and the VT-CPEM calibration are displayed in Appendix B. Furthermore, an overview of the whole framework is shown in the following Fig. 4.

2.2.2. *Vehicle simulator for EVs*

The VT-Comprehensive Power-based EV Energy consumption Model (VT-CPEM) is a backward highly-resolved power-based model. Specifically, the model requires as inputs the instantaneous speed, grade, payload on-board and the vehicle characteristics, and produces as output the energy consumption (EC) [kWh/km] by the vehicle for a specific drive cycle, the instantaneous power consumed [kW], and the State Of Charge (SOC) of the electric battery [%] at the end of the simulation. This model accurately estimates the energy consumption, producing an average error of about 6 % relative to empirical data (Fiori et al., 2016). The model first calculates the instantaneous power at the wheels $P_W(t)$ on the basis of the path (e.g. slope), trajectory (e.g. speed profile) and vehicle characteristics and after the instantaneous required traction power $P_T(t)$ is determined based on vehicle efficiencies (engine, braking system, batteries). Finally, integration of $P_W(t)$ and $P_T(t)$ over the entire duration of the driving cycle allows calculation of energy consumption/recovery and the corresponding variation of the state-of-charge, given its value at the beginning of the driving cycle.

For the sake of brevity, only the formula applied to calculate the power required for traction $P_T(t)$ is reported, as to show the 4 model parameters to be calibrated against trajectory data shown in Appendix B. Additional details on the VT-CPEM are reported in (Fiori et al., 2016).

In more detail, once calculated the power at the wheels $P_W(t)$ as reported in (Fiori et al., 2016), the power necessary to provide traction (P_T) is:

$$P_T(t) = \begin{cases} \dfrac{P_W(t)}{\eta_{DL} \bullet \eta_{EM} \bullet \eta_{BAT}} if P_W(t) \geq 0 \\ (P_W(t)) \bullet (\eta_{DL} \bullet \eta_{EM} \bullet \eta_{BAT}) \bullet \eta_{RB}(t) if P_W(t) \langle 0 \end{cases} \quad (8)$$

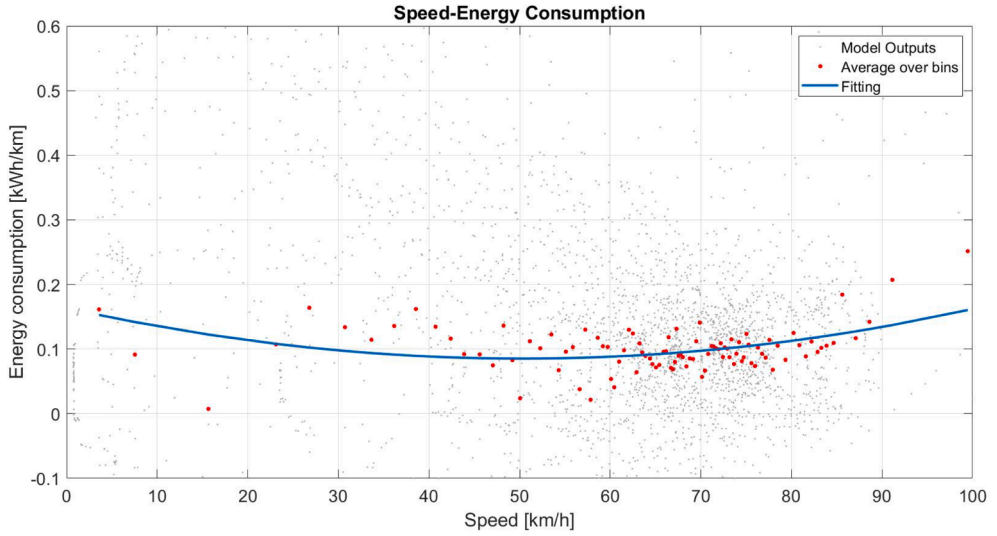

Fig. 5. Speed-Energy consumption relation for the powertrain analyzed (EV).

Table 1
Fitting of the powertrain analysed.[a]

f(x) = p1 * x^2 + p2 * x + p3	Coefficients
EV [kWh/km]	p1 = 3.102e-05
	p2 = -0.003117
	p3 = 0.1636
ICEV [l/100 km]	p1 = 7.043e-04
	p2 = -0.1452
	p3 = 13.6

[a] With x being the speed of the vehicle in [km/h].

where η_{DL} is the driveline efficiency, η_{EM} is the efficiency of the electric motor, η_{BAT} is the efficiency of the battery system and $\eta_{RB}(t)$ the regenerative braking energy efficiency. It is worth mentioning that the three efficiency parameters η_{DL}, η_{EM} and η_{BAT} are inherent characteristics of each vehicle, and they usually fall in between 0.90 and 0.98: this enables setting proper upper and lower bounds in the estimation of such efficiency parameters, as it will be described in Appendix B. On the contrary, the parameter $\eta_{RB}(t)$ is defined as a function of time t as follows, in accordance with (Fiori et al., 2016):

$$\eta_{RB}(t) = \begin{cases} e^{-\frac{\alpha}{|a(t)|}} & if a(t) < 0 \\ 0 & if a(t) \geq 0 \end{cases} \tag{9}$$

wherein the parameter α depends upon the specific vehicle under analysis and should be therefore estimated as well, usually in the [0.005,1] range. Specifically, such range is identified to comply with expected lower and upper bounds of the regenerative braking energy efficiency η_{RB}, as discussed in detail in (Fiori et al., 2016).

2.2.3. *Estimation of the link-based energy consumption function*

Running the model calibrated (as reported in the Appendix B) in a quasi-Monte Carlo framework, a macroscopic energy consumption function for each link is estimated. In particular, the relationship between average speed over a road segment and average energy consumption is calculated based on microscopic energy consumption simulated through the VP-CPEM.

Extracted trajectories reported in the Appendix B have been randomly split into 50 m-long elemental segments over each link. The random sampling has been performed in a quasi-Monte Carlo fashion by means of the low-discrepancy Sobol sequence of quasi-random numbers (Sobol, 1976). The above procedure allowed us to generate many elemental segments from the entire trajectory database. Each elemental segment has been associated with an average speed and a corresponding distribution of electric vehicle energy consumption, from which the function is estimated.

Simulated data and results of the polynomial fitting are reported in Fig. 5 and Table 1, respectively. For completeness, in the same table are also shown the values of energy consumption referred to the ICEV used for numerical applications (see Fiori et al., 2019). In more detail the energy consumption of ICEVs (l/100 km vs speed) derives from the use of CO2MPAS vehicle simulator (CO2MPAS, 2018), developed by the Joint Research Centre of the European Commission (Mogno et al., 2020; Ciuffo and Fontaras, 2017;

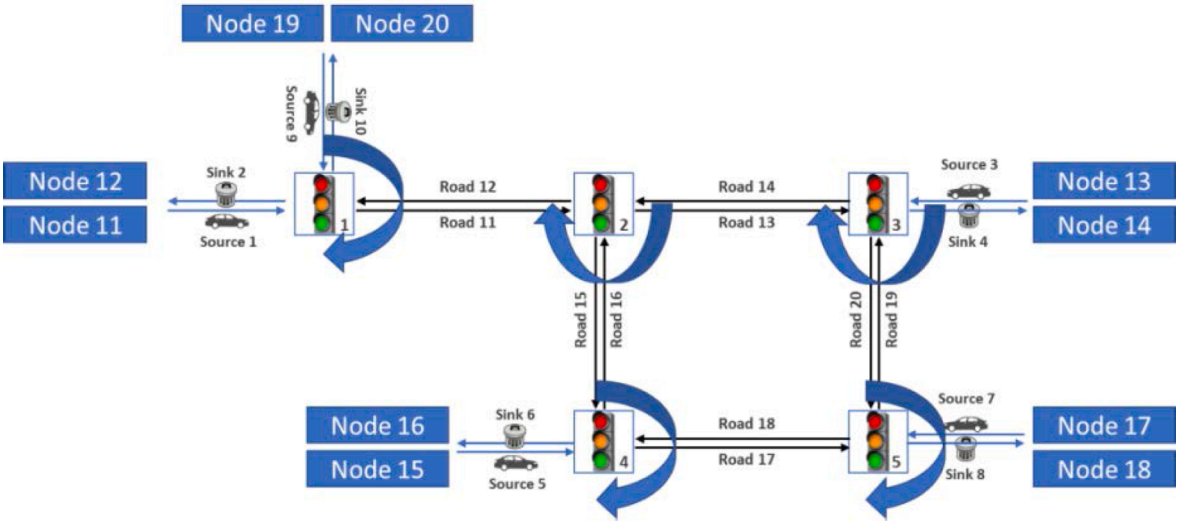

Fig. 6. Five – node grid network layout.

Table 2
Model's parameters.

Parameter	CTM	CA
Δt time step	1 s	
$\mathbf{k_{jam}}$ jam density	200 veh/km	
Cell length	22.50 m	2.50 m
Vehicle length	–	2 cells
$\mathbf{v_f}$ free flow speed	22.50 m/s	9 cells/s
w shock wave speed	5 m/s	–
$\mathbf{q_i}$ maximum flow rate	2000 veh/h	–
p dawdling probability	–	0.266
Min speed to apply dawdling	–	2 cells/s

Tsiakmakis et al.,2017; Arcidiacono et al., 2017), as specified in the paper and reported in previous studies (Fiori et al. 2019).

3. Experiment setup and numerical results

This section displays the results of two numerical applications[10]: the single-level optimization of the traffic light plans and a bi-level procedure adding speed optimization. Concerning the speed optimization, the details of the strategy, are described for sake of brevity in Appendix C.

The network used to obtain the results has five interacting junctions connected between them with single-lane links of 810 m in both directions, totaling ten internal links. It also has five origin nodes and five destination nodes (five-node grid network) connected to the network, using five external links of 300 m to connect the sources with the network,[11] and another five external links of 90 m to connect the network with the sinks. The following Fig. 6 shows a scheme of the network layout. Circular arrows at each junction represents the stage sequences that have been preliminarily evaluated trough enumeration approach (see Memoli et al., 2017). Each junction has three approaches with a green light in only one stage and an "all-red" period between stages of 3 s, the cycle length of 90 s is equal for all intersections.

The following Table 2 shows the main settings of the traffic flow model parameters The simulation horizon is equal to 4500 s, with an initial warm-up period of 900 s.

The two applications considered were performed to optimize:

- traffic lights using mono-criterion and multi-criteria approach,
- traffic lights and speeds on a bi-level iterative procedure

[10] The proposed methods were coded by the authors and developed in MATLAB (Release R2019b). All simulations were run on a computer with an Intel(R) Xeon(R) CPU E3-1245 v6 @ 3.70GHz (8 CPUs), ~3.7GHz with 8192MB RAM, and an OS Windows 10 Pro 64-bit.

[11] Thus, it is possible to model queue formation and dissipation.

Table 3
Entry – exit matrix.

		Exit [PCU/h]					
		12	14	16	18	20	Total
Entry [PCU/h]	11	0	10	10	10	0	30
	13	10	0	2	2	10	24
	15	10	2	0	2	10	24
	17	10	2	2	0	10	24
	19	0	10	10	10	0	30
	Total	30	24	24	24	30	132

Table 4
Path flow patterns.

Origin	Destination	Path ID	Arc sequence						Probability	N of vehicles per hour	N vehicles in simulation
11	14	1	{1	11	13	4	–	–}	0.9	9	11
		2	{1	11	15	17	19	4}	0.1	1	1
	16	1	{1	11	13	20	18	6}	0.1	1	1
		2	{1	11	15	6	–	–}	0.9	9	11
	18	1	{1	11	13	20	8	–}	0.5	5	6
		2	{1	11	15	17	8	–}	0.5	5	6
	20	1	{1	10	–	–	–	–}	0.5	0	0
		2	{1	10	–	–	–	–}	0.5	0	0
13	12	1	{3	14	12	2	–	–}	0.9	9	11
		2	{3	20	18	16	12	2}	0.1	1	1
	16	1	{3	14	15	6	–	–}	0.5	1	1
		2	{3	20	18	6	–	–}	0.5	1	1
	18	1	{3	14	15	17	8	–}	0.1	0	0
		2	{3	20	8	–	–	–}	0.9	2	2
	20	1	{3	14	12	10	–	–}	0.9	9	11
		2	{3	20	18	16	12	10}	0.1	1	1
15	12	1	{5	16	12	2	–	–}	0.1	1	1
		2	{5	17	19	14	12	2}	0.9	9	11
	14	1	{5	16	13	4	–	–}	0.5	1	1
		2	{5	17	19	4	–	–}	0.5	1	1
	18	1	{5	16	13	20	8	–}	0.9	2	2
		2	{5	17	8	–	–	–}	0.1	0	0
	20	1	{5	16	12	10		–}	0.9	9	11
		2	{5	17	19	14	12	10}	0.1	1	1
17	12	1	{7	19	14	12	2	–}	0.5	5	6
		2	{7	18	16	12	2	–}	0.5	5	6
	14	1	{7	19	4			–}	0.9	2	2
		2	{7	18	16	13	4	–}	0.1	0	0
	16	1	{7	19	14	15	6	–}	0.1	0	0
		2	{7	18	6			–}	0.9	2	2
	20	1	{7	19	14	12	10	–}	0.5	5	6
		2	{7	18	16	12	10	–}	0.5	5	6
19	12	1	{9	2				–}	0.5	0	0
		2	{9	2				–}	0.5	0	0
	14	1	{9	11	13	4		–}	0.9	9	11
		2	{9	11	15	17	19	4}	0.1	1	1
	16	1	{9	11	13	20	18	6}	0.1	1	1
		2	{9	11	15	6		–}	0.9	9	11
	18	1	{9	11	13	20	8	–}	0.5	5	6
		2	{9	11	15	17	8	–}	0.5	5	6

The indicators to analyze the results of the applications are defined as:

- *Total time spent (TTS):* the sum of the number of vehicles on each link for each time step during the simulation horizon over the warm-up period, obtaining a unique value for the whole network.
- *Total delay (TD):* the extra time spent by each vehicle on a link due to congestion or the presence of traffic lights, obtained as the total time spent of each vehicle on each link minus the time it would have taken to cross the link on a free-flow condition without traffic lights.
- *Consumption EV and consumption ICEV:* as the sum of the consumption of each vehicle in each link of the network considering all of them as EV or ICEV, obtained from the time to travel each link and applying the respective energy law.

Table 5
Indicators overview for EVs.

Objective function	Total Time Spent [veh s]	Consumption EVs scenario [kWh]	Total Delay[a] [s]	Final value of the Objective function
Min TTS	19810	32.71	4380	19810 [veh s]
Min sum consumption EV	28405	28.93	11786	28.93 [kWh]
Min multi-objective	22572	29.91	6341	0.41

[a] To validate the contribution of each component of the TTS (see Section 2.1.3), the TD values are evaluated separately. The results provide a further check of the trend of each term and confirm the clear contribution of both terms.

Table 6
Mean values of the specific consumption for EV.

Objective ID	Mean consumption EVs scenario* [kWh/km]		
	External links	Internal links	All network
Min TTS	0.109	0.101	0.105
Min sum consumption EV	0.097	0.088	0.092
Min multi-objective	0.100	0.092	0.095

*Computed as mean value with respect to links and vehicles.

3.1. *Traffic lights: mono-criterion and multi-criteria optimization*

Concerning traffic lights optimization, the focus is to compare mono-criterion with multi-criteria optimization, minimizing the total time spent and the total consumption considering all the vehicles in the network. The comparison is carried out for both ICEVs and EVs.

3.1.1. *Baseline scenario*

Regarding the entry-exit demand, the following Table 3 shows the considered origin–destination pair flows (baseline scenario). Further analyses about different travel demand values (high demand scenario) are shown in Section 3.1.2; it must be clarified that this paper does not analyze the impact of different travel demand profiles (deterministic vs stochastic), since these aspects will be the object of future studies.

The path choice behavior was modeled considering two paths for each o-d pair (selective approach to path choice specification) and a logit choice model. The perceived utility of each path from origin, o, to any destination, d, is assumed distributed with variance σ_0^2 equal to 20 % of average minimum path costs across all destinations. Thus, the dispersion parameter for origin o is given by $\theta_0 = \sqrt{6}/\pi \sqrt{\sigma_0^2}$. The summary of the path flow patterns is shown below (Table 4).

The results are displayed in Table 5, which shows the values of the indicators for each optimization with reference to the whole network, while Table 6 shows the mean values of the specific consumption for the vehicles in the network not only with reference to the whole network but also for the internal and the external links.[12] Results are also referred to the EVs (rate of 100 %).

The following Fig. 7 shows the traffic light plans of each intersection for the baseline scenario, considering the diverse objective functions (minimum Total Time Spent, minimum sum of EV consumption, and minimum multi-objective function).

It is possible to analyze that the ICEV and EV have different behavior: for a mono-criterion optimization based on TTS, the minimum value of consumption is also achieved for the ICEV, while it does not happen the same for EV; in this sense, the multi-criteria optimization can be considered only with the EV consumption. A further discussion is provided in the following. Regarding the characteristics of the considered traffic flow model, the max speed is equal to 22.5 m/s (81 km/h); this parameter has been set considering the realism of the representation for an urban context. Therefore, the TTS minimizes as the mean speed of vehicles approaches the fixed max speed of 81 km/h. Concerning the consumption of ICEV (shown in Section 2.2.2; for more details see Fiori et al., 2019), the experimental representation has a minimum value for a speed close to 103 km/h (see the figure below of consumption against speed for further details). Because of this, the consumption value achieved in our simulation is a feasible sub-optimal solution given the maximum speed constraint introduced in the model. Summing up, *for a mono-criterion optimization based on TTS, the minimum value of consumption is also achieved for the ICEV* can be confirmed in our case study and cannot be accepted as a general sentence.

Finally, the landscape of the EV consumption against speed has a minimum for a speed close to 50 km/h, within the maximum speed set on the traffic flow model (see figure below). Thus, the results highlight that the minimisation of TTS provides higher values of EV consumption than those obtained for the direct consumption minimisation. The trend of the mean speed of vehicles in each link also confirms these results.

Furthermore, using the multi-criteria optimization to compare, the indicators worsen from each mono-criteria optimization of around 12 % for the TTS and 3 % of the EV's Consumption. Comparing the results of the mono-criterion optimizations, when

[12] External links: (1–3–5–7–9) from sources to the network, and (2–4–6–8–10) from the network to the sinks. Internal links: (11–20) that connect the nodes of the network.

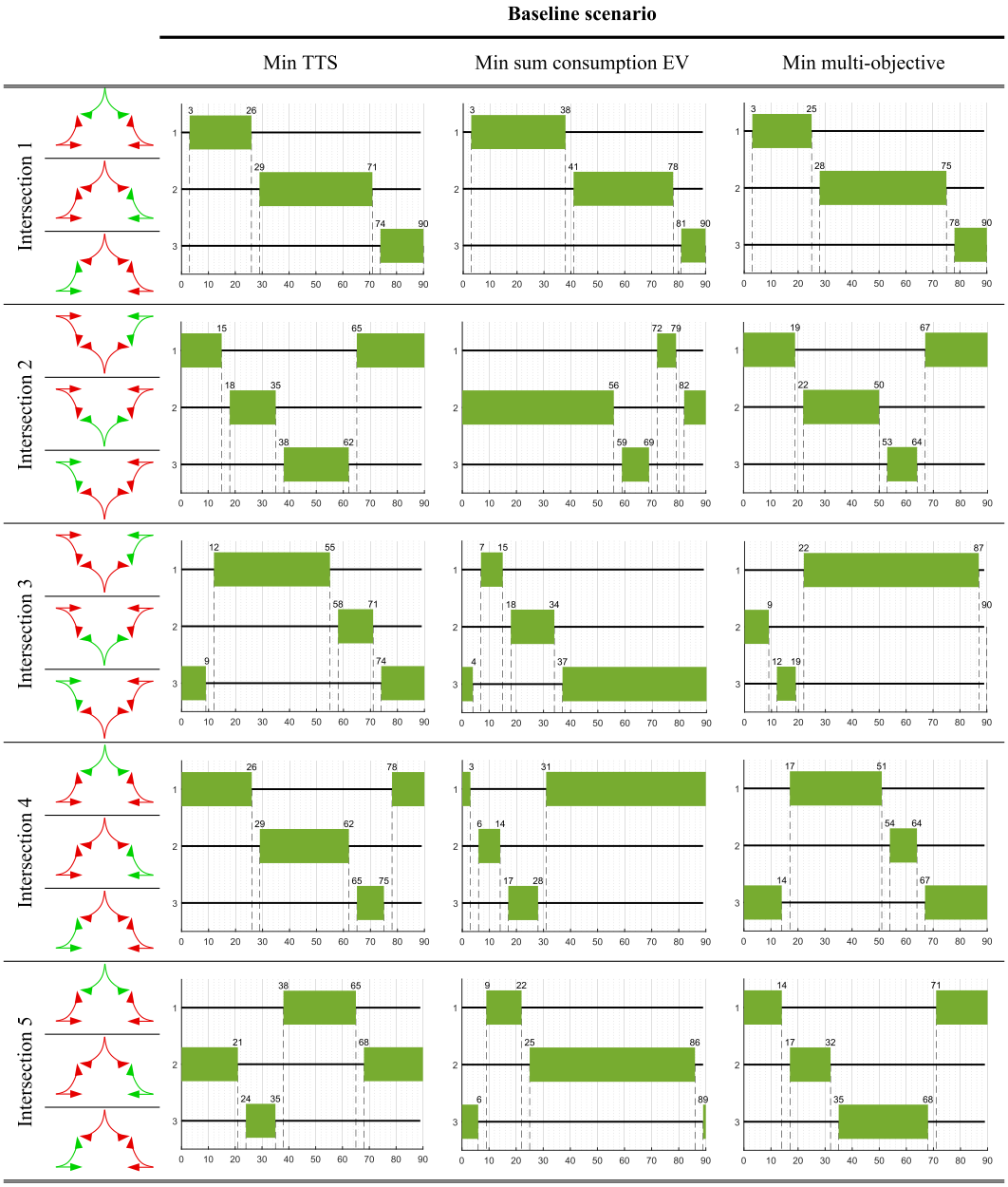

Fig. 7. Traffic light plans (in seconds) on the baseline scenario for the different objective functions.

minimizing the TTS, the value of EV consumption is around 12 % higher than its minimum value. Meanwhile, when minimizing the EV consumption, the TTS value is near 30 % higher than its minimum value found. Comparing the value of the performance indicator waiting time to its minimum found, it is around 63 % higher for the minimization of the EV consumption while is near 32 % higher for the multi-criteria optimization.

Furthermore, to highlight the effectiveness of the optimization procedure, the following Fig. 9a displays the landscapes of the objective function considered in the multi-criteria optimization (comparing the trajectories of the mean value and the best values) against the number of iterations. Fig. 9b shows the EV consumption versus the TTS for some iterations, with its values normalized from the minimum and the maximum values achieved during the optimization procedure. The first Figure highlights an asymptotic convergence achieved around iteration 750, also confirmed by Fig. 9b; in more detail, it is possible to observe that the procedure converges to the optimal solution around iteration 1500.

In Fig. 10, the indicator of the total energy consumption of all vehicles on the total distance travelled against the link length is shown. Thus, a high value of it may depend, for each link, on a high number of vehicles with a low value of consumption and vice-versa on a low number of vehicles but with a higher value of consumption. For completeness, as already anticipated in the preliminary

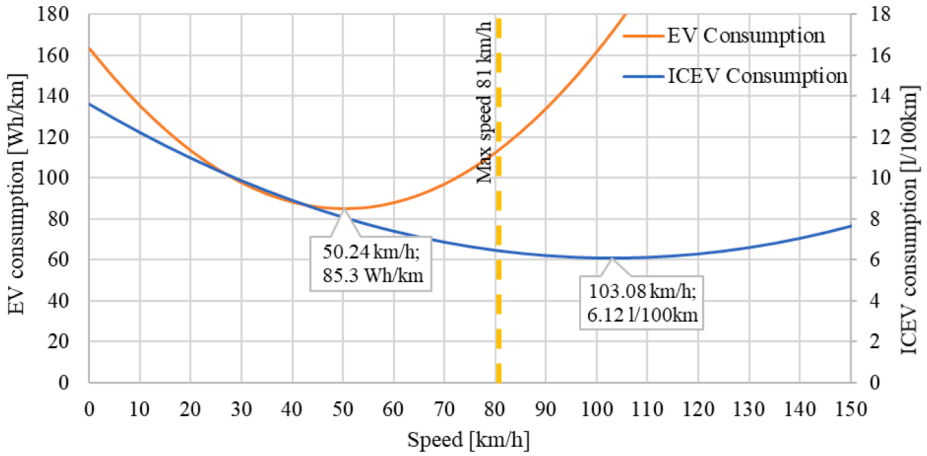

Fig. 8. EV/ICEV consumption against Speed.

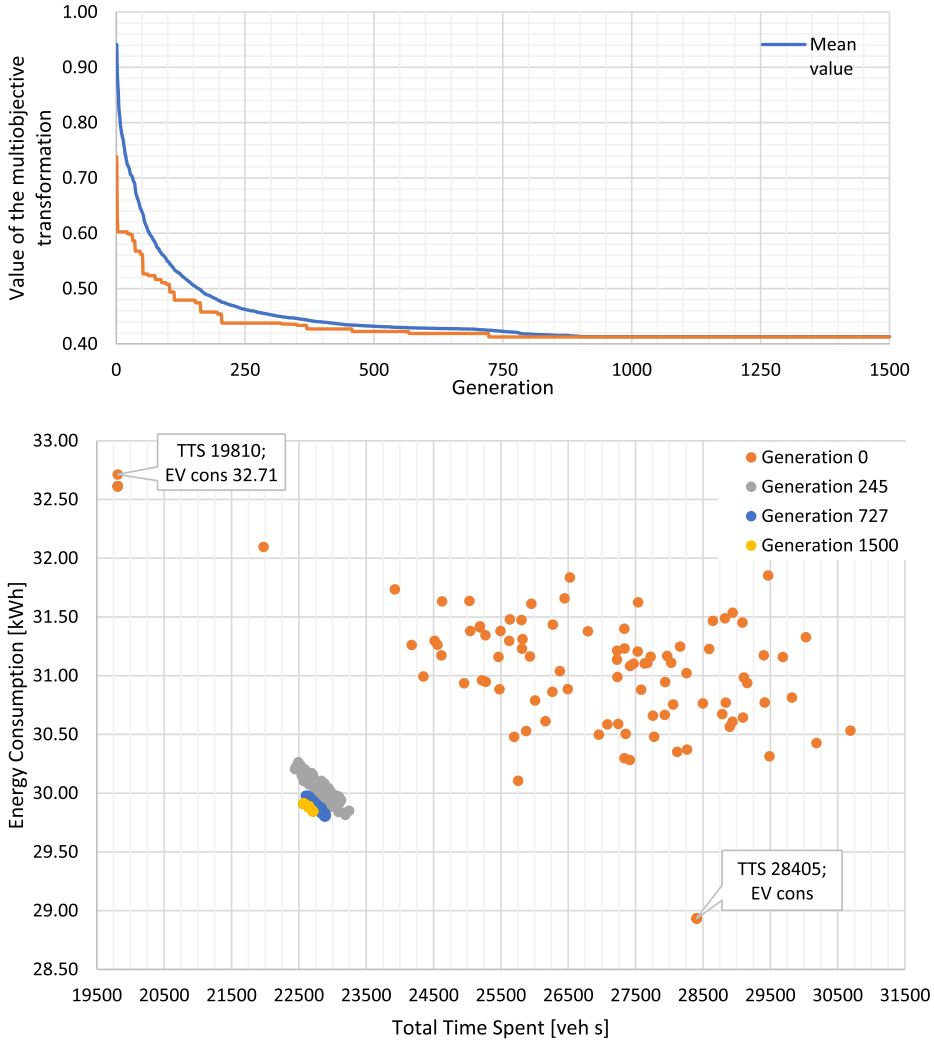

Fig. 9. (a) Transformed value of the multi-objective function at each generation number. (b) Energy consumption against total time spent.

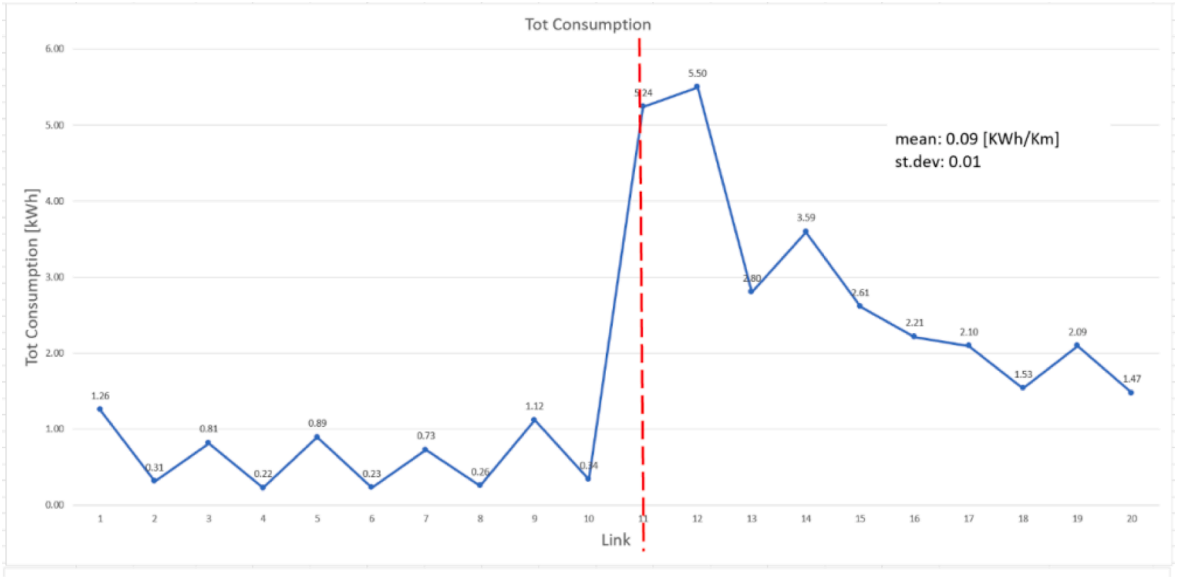

Fig. 10. the total energy consumption of all vehicles on the total distance travelled against the link identification [internal links are from 11 to 20; external entering links are 1, 3, 5, 7, 9 and external exiting links are 2, 4, 6, 8 and 10].

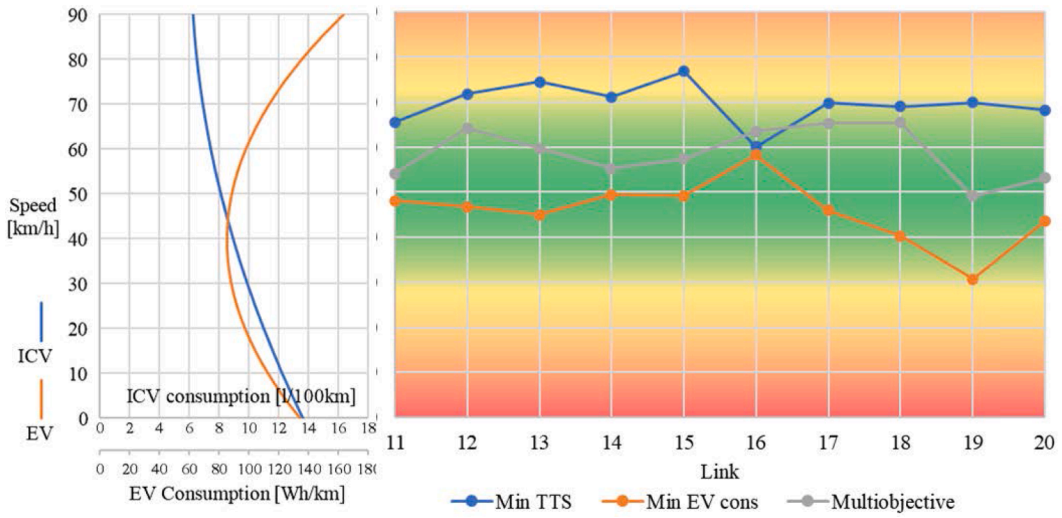

Fig. 11. (a) Speed against EV/ICEV consumption; (b) Speed against link.

description of the case study, the lengths are 300 m for links 1–3–5–7–9 (sources to network), 90 m for links 2–4–6–8–10 (network to sinks) and 810 m for links from 11 to 20 (inner links of the network). On the same figure, as a further analysis, the mean value and the standard deviation of the energy consumption are shown, considering the analytical expressions used to calculate the indicators for the vehicle i on link l. In this analysis, the standard deviations of the total consumption is low, highlighting that the traffic flow model is consistent with the adopted formulation for the consumption estimation. Given the specific application of the proposed case study and the advantages in terms of simulation efforts, the traffic model adopted represents the best solution for such application also in combination with the polynomial correlation between energy consumption and speed.

Furthermore, in Fig. 10, (that is the total energy consumption averaged on vehicles number against the link length) is shown that the main contribution in the computation of the total consumption indicator is given by links 11, 12 and 14 since the number of vehicles on these links is higher than the other links, and a lower contribution by the other internal links. Concerning the external links 1–3–5–7–9 that connect the sources with the network, they have a higher length than the other external links (300 m versus 90 m) and have traffic lights at the end of the link affecting their travel times, increasing them.

Finally, the speed contribution on the consumption indicator, is highlighted through the following Fig. 11.

The results concerning the internal links have been analyzed to evaluate the strategy effectiveness. It is possible to observe that, as

Table 7
Entry – exit matrix.

		Exit [PCU/h]					
		12	14	16	18	20	Total
Entry [PCU/h]	11	0	100	50	50	0	200
	13	50	0	50	50	50	200
	15	50	20	0	20	50	140
	17	50	20	20	0	50	140
	19	0	50	50	50	0	150
	Total	150	190	170	170	150	830

Table 8
Path flow patterns.

Origin	Destination	Path ID	Arc sequence						Probability	N of vehicles per hour	N vehicles in simulation	N of vehicles per hour	N vehicles in simulation
										Baseline		More Flow	
11	14	1	{1	11	13	4	–	–}	0.9	9	11	90	113
		2	{1	11	15	17	19	4}	0.1	1	1	10	12
	16	1	{1	11	13	20	18	6}	0.1	1	1	5	6
		2	{1	11	15	6	–	–}	0.9	9	11	45	56
	18	1	{1	11	13	20	8	–}	0.5	5	6	25	31
		2	{1	11	15	17	8	–}	0.5	5	6	25	31
	20	1	{1	10	–	–	–	–}	0.5	0	0	0	0
		2	{1	10	–	–	–	–}	0.5	0	0	0	0
13	12	1	{3	14	12	2	–	–}	0.9	9	11	45	56
		2	{3	20	18	16	12	2}	0.1	1	1	5	6
	16	1	{3	14	15	6	–	–}	0.5	1	1	25	31
		2	{3	20	18	6	–	–}	0.5	1	1	25	31
	18	1	{3	14	15	17	8	–}	0.1	0	0	5	6
		2	{3	20	8	–	–	–}	0.9	2	2	45	56
	20	1	{3	14	12	10	–	–}	0.9	9	11	45	56
		2	{3	20	18	16	12	10}	0.1	1	1	5	6
15	12	1	{5	16	12	2	–	–}	0.1	1	1	5	6
		2	{5	17	19	14	12	2}	0.9	9	11	45	56
	14	1	{5	16	13	4	–	–}	0.5	1	1	10	12
		2	{5	17	19	4	–	–}	0.5	1	1	10	12
	18	1	{5	16	13	20	8	–}	0.9	2	2	18	23
		2	{5	17	8	–	–	–}	0.1	0	0	2	2
	20	1	{5	16	12	10		–}	0.9	9	11	45	56
		2	{5	17	19	14	12	10}	0.1	1	1	5	6
17	12	1	{7	19	14	12	2	–}	0.5	5	6	25	31
		2	{7	18	16	12	2	–}	0.5	5	6	25	31
	14	1	{7	19	4			–}	0.9	2	2	18	23
		2	{7	18	16	13	4	–}	0.1	0	0	2	2
	16	1	{7	19	14	15	6	–}	0.1	0	0	2	2
		2	{7	18	6			–}	0.9	2	2	18	23
	20	1	{7	19	14	12	10	–}	0.5	5	6	25	31
		2	{7	18	16	12	10	–}	0.5	5	6	25	31
19	12	1	{9	2				–}	0.5	0	0	0	0
		2	{9	2				–}	0.5	0	0	0	0
	14	1	{9	11	13	4		–}	0.9	9	11	45	56
		2	{9	11	15	17	19	4}	0.1	1	1	5	6
	16	1	{9	11	13	20	18	6}	0.1	1	1	5	6
		2	{9	11	15	6		–}	0.9	9	11	45	56
	18	1	{9	11	13	20	8	–}	0.5	5	6	25	31
		2	{9	11	15	17	8	–}	0.5	5	6	25	31

expected, the EV consumption indicator is minimized when chosen as the objective function to optimize. The multi-objective optimization provides intermediate results of EV consumption between those of the two other objective functions. These results are different when analyzing ICEV since the TTS minimization for the ICEV also gives the lowest value of its consumption, compared to the other objective functions, since the mean speed of vehicles is closer to the minimum of the consumption-speed relationship used. However, it is not possible to approach the global minimum of ICEV consumption as the maximum speed of the traffic model is not consistent with the optimal speed that minimizes the ICEV consumption, considering an urban context.

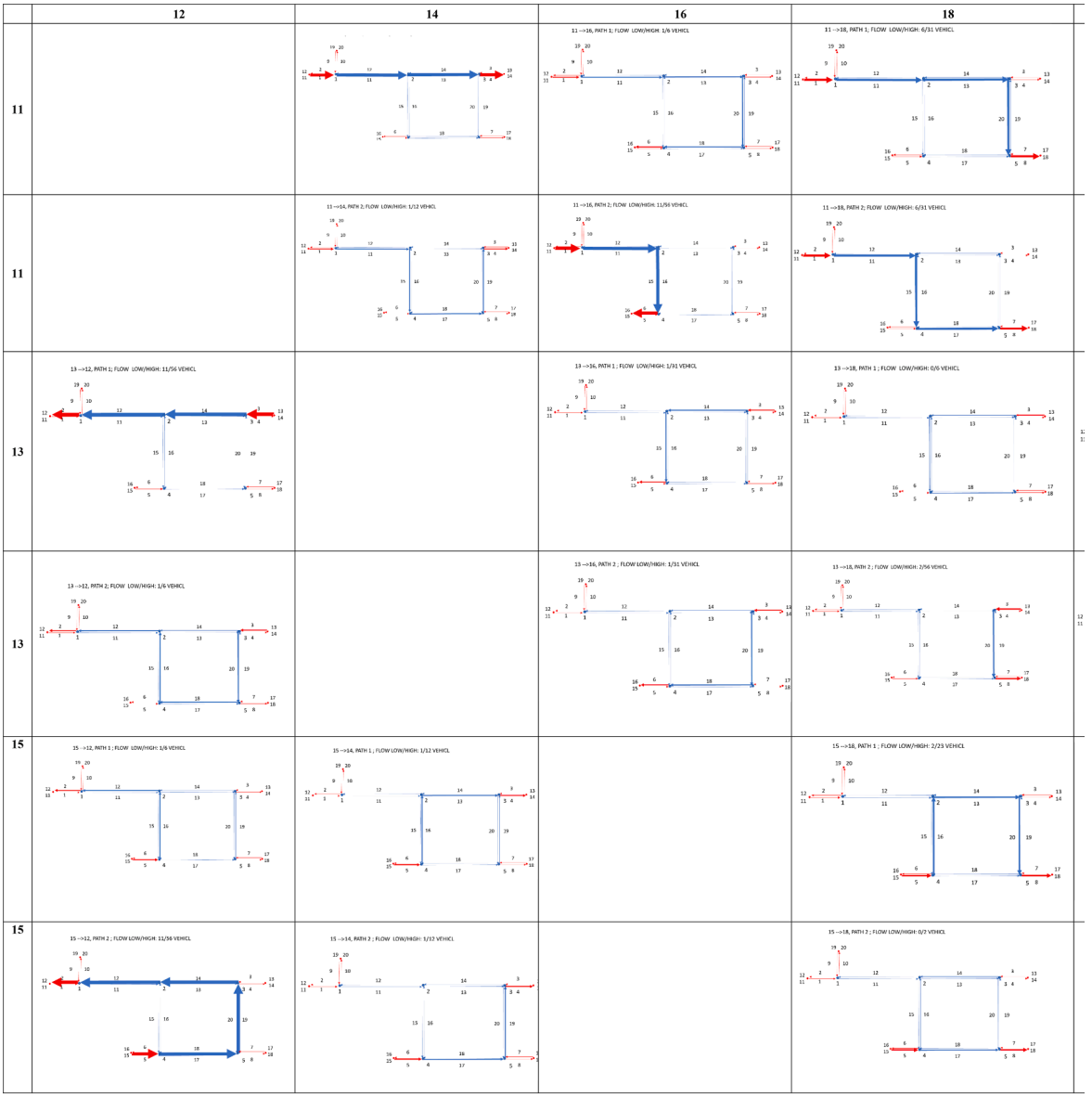

Fig. 12. origin – destinations paths.

3.1.2. High demand scenario

This section aims at discussing the results of further analyses about different travel demand values. The details about the experimental setup and the numerical applications are discussed in the following.

In particular, regarding the entry-exit demand, the following Table 7 shows the considered origin–destination pair flows. Table 8 shows the summary of the path flow patterns; Fig. 12 shows the origin – destination paths,[13] while Fig. 13 shows the path flow patterns diagrams.

In terms of numerical applications, the focus is to compare mono-criterion with multi-criteria optimization, minimizing the total time spent and the total consumption considering all the vehicles in the network (as ICEVs and EVs). The results are displayed in Table 9, which shows the values of the indicators for each optimization with reference to the whole network. As already discussed in Section 3.1, it is possible to analyze that the ICEV and EV have different behavior: for a mono-criterion optimization based on TTS, the minimum value of consumption is also achieved for the ICEV, while it does not happen the same for EV; in this sense, the multi-criteria

[13] The figure also shows the flows in low and high demand scenarios.

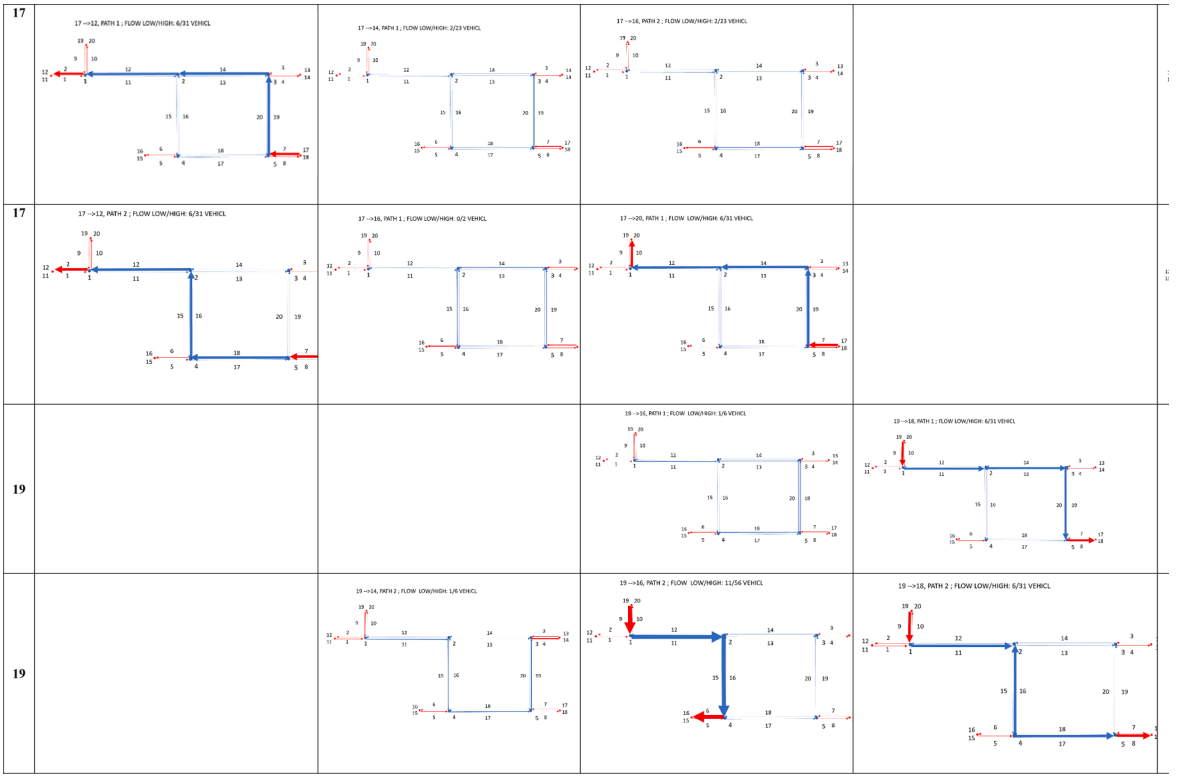

Fig. 12. (*continued*).

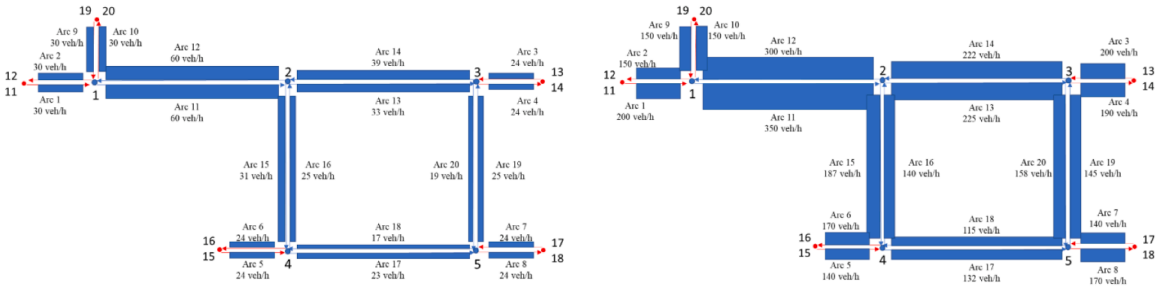

Flow pattern – low demand

Flow pattern – high demand

Fig. 13. path flow patterns.

Table 9
Results overview.

Objective function	Total Time Spent [veh s]	Consumption EV scenario [kWh]	Total Delay [s]	Final value of the Objective function
Min TTS	126424	194.31	31697	126,424 **[veh s]**
Min sum consumption EV	748006	161.75	346914	161.75 [kWh]
Min multi-objective	242221	170.64	141887	0.34

optimization can be considered only with the EV consumption.

Table 10 makes it possible to compare the green splits and the absolute offsets of the baseline and the high demand scenario obtained regarding each one of the three objective functions (Total Time Spent - TTS, EV energy consumption - EC, and multi-objective).

The following Fig. 14 shows the traffic light plans of each intersection for the high demand scenario, considering the diverse objective functions (minimum Total Time Spent, minimum sum of EV consumption, and minimum multi-objective function).

Table 10
Green times (in seconds) for each scenario and each objective function.

		Low Demand Scenario			High Demand Scenario		
		Min TTS	Min sum cons. EV	Min multi-objective	Min TTS	Min sum cons. EV	Min multi-objective
Intersection 1	Offset	0	0	0	0	0	0
	Green Stage 1	23	35	22	21	45	31
	Green Stage 2	42	37	47	38	18	42
	Green Stage 3	16	9	12	22	18	8
Intersection 2	Offset	62	69	64	61	88	67
	Green Stage 1	40	7	42	25	65	12
	Green Stage 2	17	64	28	15	9	53
	Green Stage 3	24	10	11	41	7	16
Intersection 3	Offset	9	4	19	7	23	52
	Green Stage 1	43	8	65	27	7	59
	Green Stage 2	13	16	9	16	10	9
	Green Stage 3	25	57	7	38	64	13
Intersection 4	Offset	75	28	14	65	52	27
	Green Stage 1	38	62	34	42	39	63
	Green Stage 2	33	8	10	27	7	8
	Green Stage 3	10	11	37	12	35	10
Intersection 5	Offset	35	6	68	33	5	12
	Green Stage 1	27	13	33	36	25	14
	Green Stage 2	43	61	15	20	37	37
	Green Stage 3	11	7	33	25	19	30

Given the analytical expressions of the two objective functions (Equations (1) and (5)), it is expected that the TTS objective function during the optimization will be more sensitive to the number of vehicles than the EC objective function. Indeed, the TTS strictly depends on the number of vehicles, while the EC is a concave function to their speed. Concerning the timing plans composition, higher values of green splits are expected for the approaches with a greater number of vehicles (see Fig. 13), especially in the case of TTS optimization, allowing for throughput of vehicles maximization. Furthermore, in the case of TTS optimization, the traffic signals plans can be very similar even in the presence of two different demand levels and the absolute offsets do not change significantly when comparing high and low demand scenarios. With reference to the EC objective function, slightly different considerations must be done. Due to the concave trajectory of the energy consumption function of Evs (see Fig. 8), this objective function aims at achieving a 'target' value of the mean speed. Indeed, during the optimization, it may be necessary to either increase or decrease the mean speed of vehicles, by adjusting not only the green times but mainly the offsets. As a result, in the case of EC optimization, the traffic lights plans (green splits and offsets values) may be different between the high and low demand scenarios. In conclusion, the optimization procedure assigns higher values of green splits to the approaches with more traffic, this is evident in low and high demand scenarios, especially in the case of TTS optimization. Additionally, given the analytical expression of the objective functions, it is expected to obtain different traffic lights plans between the TTS and EC, while also within EC optimization by increasing the demand (low vs high demand scenario). Results also highlight the impact of both criteria in multi-objective optimization. Finally, the complex layout that is a network composed of interacting junctions, has a significant effect on the optimization especially in the case of EC objective function.

3.2. Bi-level optimization: Traffic lights (mono-criterion optimization) and speed optimization

This subsection shows the results of the bi-level iterative optimization. At the first step, the procedure starts with the TTS minimization (mono-criterion optimization) by varying the green times and the offsets of the traffic light plans. Then, the vehicles' speed near the intersections is varied with the current traffic light plans aiming to minimize the EV energy consumption. This procedure continues until it reaches the minimum Euclidean distance of both indicators (see Table 11; the optimal value is achieved at second iteration; see results in bold).

Table 11 shows the value of the indicators for each iteration. In this table, it is possible to observe that applying the speed optimization procedure gives the best solution that increases the value of the indicators from their separate minimum: around 18 % in terms of TTS and near 8 % of EV consumption. These results point out that the multi-objective optimization outperforms the speed optimization since the TTS is around 5 % worse whilst the EV energy consumption is near 4 % worse.

4. Conclusions and research prospects

The main goals of this study are as follows: (i) the development of a multi-objective optimization including the EV EC optimization that has been specified and applied, and (ii) the application of this methodology for different powertrain vehicles categories, ICEVs, and EVs.

The proposed multi-objective optimization framework, which aims at minimizing the TTS and EC of EVs, is composed of three models: (1) the traffic control model aimed at designing the traffic light decision variables; (2) the traffic flow model for the estimation of TTS as a network performance indicator, and (3) the EV model for the estimation of a specific EC at the intersections.

The optimization framework was implemented on a nine-node network where once the vehicles approach the control zone, they are

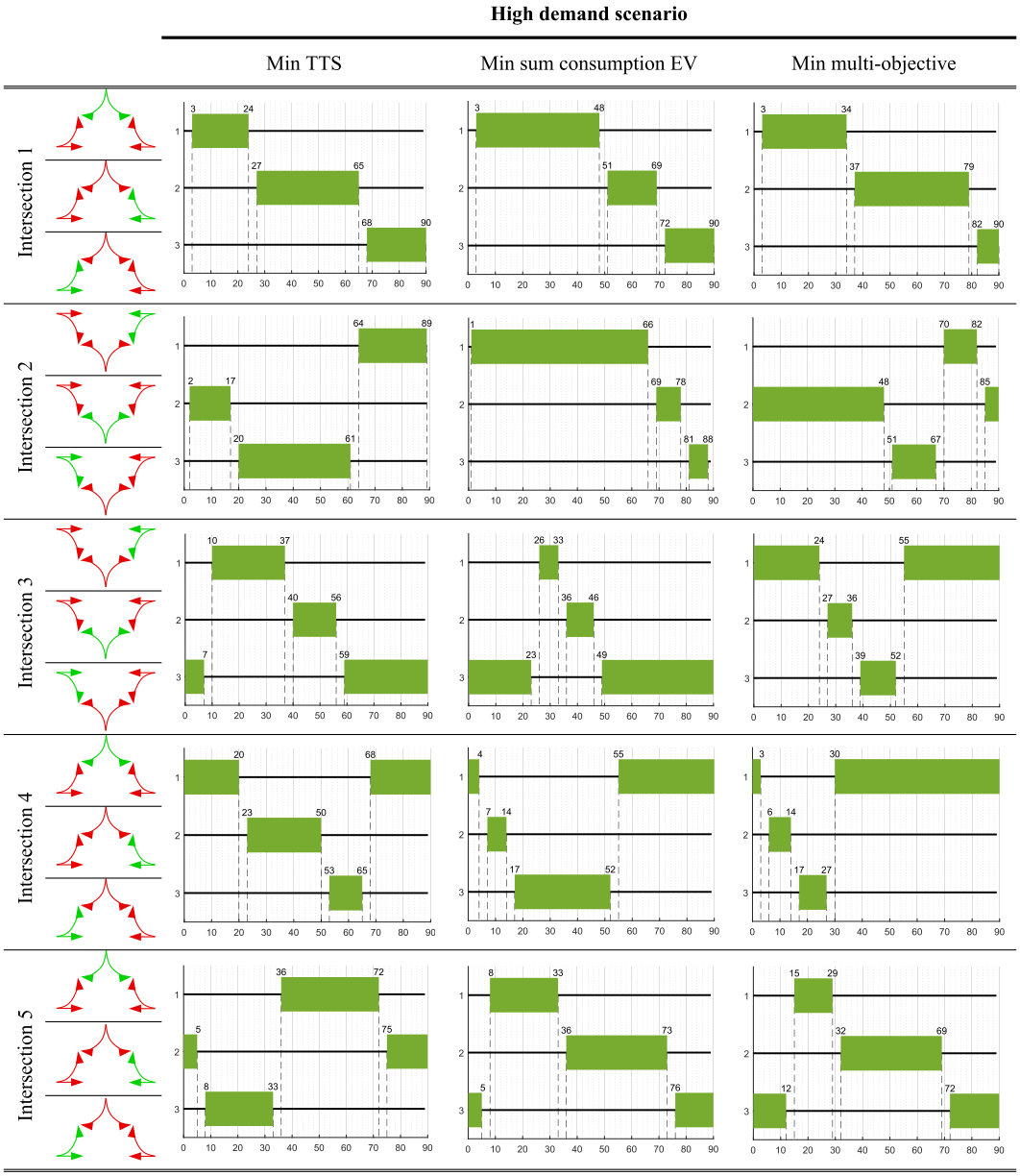

Fig. 14. Traffic light plans (in seconds) on the high demand scenario for the different objective functions.

assumed to be fully connected, and information can be exchanged between each vehicle and the traffic signal controller. Real data on individual trajectories at signalized intersections were used to calibrate the VT-CPEM model (Fiori et al., 2016) adopted to develop a link-based macroscopic energy consumption function for EVs derived from microscopic data.

In more detail, numerical simulations were carried out considering a 100 % EV rate and considering a low demand (baseline scenario). The results highlighted that the ICEV and EV have different behaviors; for the mono-criterion optimization based on TTS, the minimum value of consumption was achieved by the ICEV, while this was not observed for the EVs; in this sense, the multi-criteria optimization can only be considered for the EV consumption.

Furthermore, using the multi-criteria optimization for comparison, the indicators worsened for each mono-criteria optimization of approximately 12 % for the TTS and 3 % for the EV consumption. Comparing the results of the mono-criterion optimizations, when TTS is minimized, the EV consumption was approximately 12 % higher than its minimum. Meanwhile, when minimizing the EV consumption, the TTS was approximately 30 % higher than its minimum.

Comparing the waiting time performance indicator to its minimum, it was approximately 63 % higher for the minimization of the EV consumption, while it was nearly 32 % higher for the multi-criteria optimization.

Further analyses about different travel demand values (high demand scenario) have been carried out. In this case results confirm

Table 11
Overview of the results of the bi-level optimization.

Total Time Spent [veh s]	Consump EV [kWh]	Total Delay [s]	Distance to min TTS [adim]	Distance to min cons EV [adim]	Vector distance [adim]	Min desired [cell/s]	Desired speed [cell/s]	Max desired [cell/s]	Criterion	Iteration
19810	32.71	4380	0.00	1.00	1.00	9	9	9	Min TTS	0
25727	30.57	5166	1.00	0.00	1.00	3	3	6	Min EV Cons	0
22016	31.93	2901	0.37	0.63	0.74	3	3	6	Min TTS	1
22043	31.83	2891	0.38	0.59	0.70	3	3	11	Min EV Cons	1
21252	31.74	2650	0.24	0.55	0.60	3	3	11	Min TTS	2
23481	**31.21**	**4072**	**0.62**	**0.30**	**0.69**	**3**	**3**	**7**	**Min EV Cons**	**2**
21722	32.24	2842	0.32	0.78	0.85	3	3	7	Min TTS	3
22773	31.95	3682	0.50	0.64	0.82	3	3	6	Min EV Cons	3

that the ICEV and EV have different behavior: for a mono-criterion optimization based on TTS, the minimum value of consumption is also achieved for the ICEV, while it does not happen the same for EV.

In terms of traffic lights plans, further considerations can be made by comparing the results of low (baseline scenario) and high demand scenarios. In particular, depending on the analytical expression of the TTS and EC objective functions, different results are achieved. In more detail concerning the TTS optimization, the traffic signals plans can be very similar even in the presence of two different demand levels and the absolute offsets do not change significantly when comparing high and low demand scenarios; different traffic lights plans between the TTS and EC can be observed, while also within EC optimization by increasing the demand (low vs high demand scenario). Results also highlight the impact of both criteria in multi-objective optimization. Finally, the complex layout that is a network composed of interacting junctions, has a significant effect on the optimization, especially in the case of EC objective function.

Additionally, by applying the speed optimization procedure, the best solution had an increase in the value of the indicators from their minimums: approximately 18 % for the TTS and nearly 8 % for the EV consumption. These results indicate that the multi-objective optimization outperforms the speed optimization because the TTS and EV energy consumption of the speed optimization were approximately 5 % and 4 % worse, respectively.

In future studies, the authors plan to further investigate the integration of the proposed multi-objective optimization framework with speed by considering the enhanced traffic flow model in terms of vehicle automation (Pan et al., 2021; Jiang et al., 2021). Furthermore, the following are also areas of interest:

i) sensitivity analysis for different demand profiles (i.e., deterministic vs stochastic);
ii) to consider different penetration rates of EVs by combining the impact of EVs with the presence of conventional ICEVs;
iii) to further develop the traffic lights optimization also including the stage sequences as decision variables;
iv) to consider the application of the proposed framework to more complex intersection layouts.

CRediT authorship contribution statement

Roberta Di Pace: Conceptualization, Methodology, Writing – original draft, Writing – review & editing, Software, Validation, Formal analysis, Investigation, Data curation, Visualization, Project administration. **Chiara Fiori:** Conceptualization, Methodology, Writing – original draft, Writing – review & editing, Software, Validation, Formal analysis, Investigation, Data curation, Visualization, Project administration. **Facundo Storani:** Writing – original draft, Writing – review & editing, Software, Validation, Data curation, Visualization. **Stefano de Luca:** Writing – original draft, Writing – review & editing, Supervision, Project administration. **Carlo Liberto:** Resources, Funding acquisition, Writing – review & editing. **Gaetano Valenti:** Resources, Funding acquisition, Writing – review & editing.

Declaration of Competing Interest

The authors declare that they have no known competing financial interests or personal relationships that could have appeared to influence the work reported in this paper.

Acknowledgments

This research was partially funded by the Italian program PON AIM – Attraction and International Mobility, Linea 1 (AIM1877579-3-CUPD44I18000220006), by a research grant under the 5-years Italian programme 'Dipartimenti Universitari di Eccellenza no. 232/2016 – Legge di Bilancio 2017', CUP E65D18000820006, by the University of Salerno, under local grants no. ORSA165221 – 2016 and no. ORSA180377 – 2018. Additionally, this research was also partially funded by the "Piano Triennale della Ricerca nell'ambito del Sistema Elettrico Nazionale 2019-2021" (MiSE). Authors wish to thank anonymous reviewers for their helpful comments.

Appendix A

A.1. Traffic flow model

The general architecture of the proposed hybrid model consists of the combination of a macroscopic CTM with a meso-microscopic CA for each link (see Fig. 15). The CA is used to model the traffic flow at disaggregate level at the junction, whereas the CTM models the traffic flow at aggregate level along the link. The transitions from CA to CTM and vice versa are based on the introduction of a transition zone. Both models have the same simulation time step equal to 1 s, to obtain a consistent queuing formation and backend propagation of the congestion.

Prior to an in/depth description of the transition zone, where the two models coexist at the interfaces, some information about the main variables' definition are provided.

Concerning the Cell Transmission Model, the main variables are.

- k_i density in cell i;
- k_j jam density;
- Q_i maximum flow rate in cell i;
- V_f free flow speed;
- ω shock wave speed in congested traffic;
- Δx cell length;
- Δt time step;
- Y_i flow exiting the boundary of cell i.

Concerning the CA - Nagel-Schreckenberg Model the main variables are.

- vehicle i on the road,
- $v_i(t)$ vehicles speed
- $x_i(t)$ vehicles position
- gap g_i between vehicles

The model also contains a stochastic component called the dawdling probability in which with a probability p a vehicle can remain at the same speed (if it was accelerating) or decelerate. This allows us to model stop-and-go waves in congested traffic, varying the flow-density relation as well.

Since a link is modelled with two different aggregation levels, two transition zones have to be specified: from CA to CTM (microscopic to macroscopic) and from CTM to CA (macroscopic to microscopic).

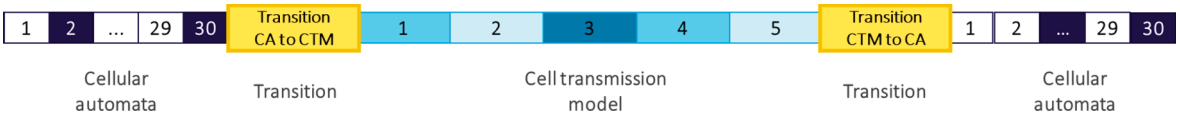

Fig. 15. Example of a link with a hybrid approach.

A.1.1. From CA to CTM – Transition 1

This transition receives vehicles from the Cellular Automata upstream, to then insert a flow into the Cell Transmission Model downstream, as can be seen in Fig. 16.

The transition zone has two subsections, one for each model:

- The macroscopic CTM section is a single cell with the same properties as the cells of the CTM model, but with a length Δx_{CTM-T1} equal to $\Delta x_{CTM} \cdot (\Delta t / Q_{CTM})$. If the cell is shorter than this value, the number of time steps t required to move the density that represents a single vehicle to the downstream cell on a free flow condition would cause that $V_f \cdot t > \Delta x_{CTM-T1}$. In order to have coherence between the length of the CTM section and the cells of the CTM model, the value $(\Delta t / Q_{CTM})$ can be rounded to the next greater integer via a ceiling function $\lceil \Delta t / Q_{CTM} \rceil$.
- The meso-microscopic CA section is an extension of the upstream CA link, with a number of cells equal to the maximum speed (i.e. the minimum gap between vehicles, hence an upstream vehicle affects a downstream one), and with the same properties, parameters and rules as the CA model.

For each time step, before a vehicle in the CA model upstream can enter the microscopic section of the transition model, it is

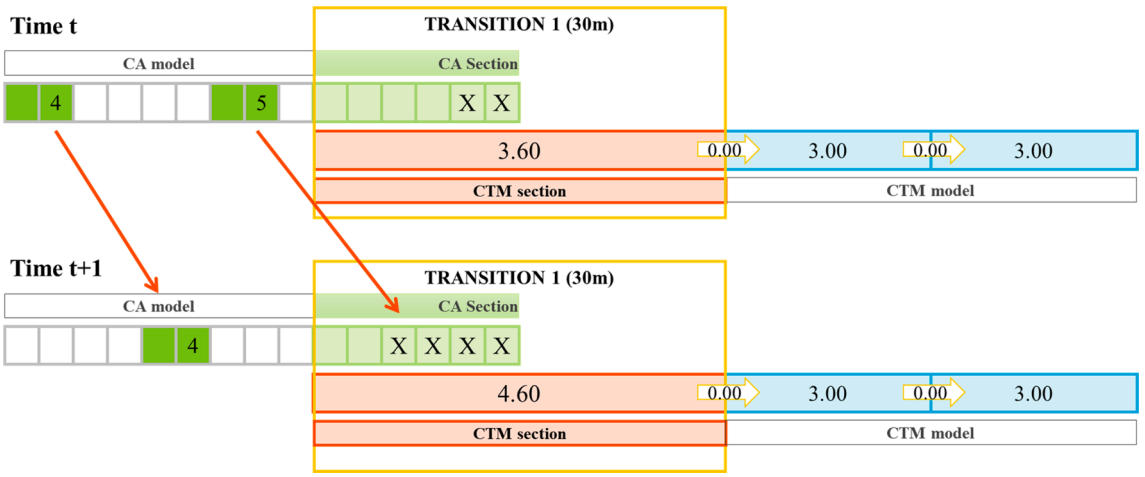

Fig. 16. Transition from CA to CTM, considering a vehicle in CA occupies 2 cells. The numbers in the CA cells are the speeds of the vehicles, while the values on the CTM cells are the number of vehicles.

necessary to calculate the available space of the transition zone, considering the CA section and the CTM section. To this end, the current number of vehicles on the macroscopic section is subtracted from the maximum number of vehicles (considering the jam density). This means that the transition zone is not jammed and has sufficient space to allocate to the incoming vehicle. The initial cells of the microscopic CA section are then declared "empty" and thus an incoming vehicle from the CA model can enter, calculating the gap (number of empty cells downstream), to then apply the normal procedure of the CA algorithm.

Length of the macroscopic CTM section.

$$\Delta x_{CTM-T1} = \Delta x_{CTM} \cdot \lceil \Delta t / Q_{CTM} \rceil \tag{10}$$

Number of vehicles in the transition section.

$$n_{veh-T1} = k_{CTM-T1} \cdot \Delta x_{CTM-T1} \tag{11}$$

Number of vehicles that can enter the transition section.

$$n^{enter}_{veh-T1} = (k_j - k_{CTM-T1}) \cdot \Delta x_{CTM-T1} \tag{12}$$

Number of cells available in the microscopic CA section ("empty" cells):

$$n_{cellsCA-T} = \frac{n^{enter}_{veh-T}}{\Delta x_{CA}} \tag{13}$$

Space gap of the vehicle upstream to the transition:

$$g_i(t) = x_{lastcellofCAmodel} - x_i(t) + n_{cellsCA-T} \tag{14}$$

After this procedure, the rules of the CA model are applied to the vehicle upstream, considering the gap with the available cells of the CA section of the transition. Then, if the position of the vehicle $x_i(t+1)$ lies within the CA section of the transition, the CTM section of the transition of the successive time step is updated.

The flow of vehicles moving through the boundary between the cell of the CTM section of the transition and the first cell of the CTM model is obtained following the same procedure as in the CTM model as described above.

A.1.2. From CTM to CA – Transition 2

The transition from the Cell Transmission Model to the Cellular Automata has a similar layout to the first, which has a length equal to the first transition with two subsections:

- A macroscopic CTM cell, with the same characteristics as the CTM model, which acts as a cell to accumulate flow,
- A microscopic CA section, of length equal to the CTM cells, which fulfils the *Courant-Friedrich-Lewy* condition ($V_f \Delta t \leq \Delta x$), to then continue with the initial segment of the CA model downstream.

A scheme of the transition cell in question can be seen in Fig. 16.

The flow $Y_{end}(t)$ of the boundary between the last cell of the CTM upstream and the macroscopic CTM cell of the transition, is calculated following the same procedure described above for the CTM model, but bearing in mind that the maximum flow that can be received (the *supply*) is also conditioned by the total number of vehicles n_{CA-T2} located in the CA component of the transition zone:

$$1S_{CTM-T2}(t) = \min\left(Q_{CTM}, \omega \cdot \left(k_j - \left(k_{CTM-T2} + n_{CA-T2}/\Delta x_{CTM}\right)\right)\right) \tag{15}$$

$$Y_{end}(t) = \min\left(D_{end}(t), S_{CTM-T2}(t)\right) \tag{16}$$

The density of the macroscopic CTM cell of the transition is then updated, considering only the incoming flow.

$$k_{CTM-T2}(t+1) = k_{CTM-T2}(t) + \left[Y_{end}(t)\right] \cdot \frac{\Delta t}{\Delta x} \tag{17}$$

If the macroscopic CTM cell of the transition has a density such that an entire vehicle is located within the cell, then it is transferred towards the microscopic CA section. To this end, the density of the CTM cell is reduced, and, if there is no other vehicle in the CA component of the transition, the status of the last available cell of the microscopic CA section is changed to "occupied", initially considering a speed equal to the desired free flow speed v_0. However, if there is another vehicle in the CA component of the transition, the new vehicle is inserted in the microscopic CA section leaving a gap equal to the speed of the first vehicle downstream, with the same speed as it can be seen in Fig. 16. The same rules as in the CA model are then applied to this vehicle. Thus, its speed and position are updated for the following time step considering the gap with an eventual vehicle downstream.

$$if\ \left(k_{CTM-T2}(t) \cdot \Delta x_{CTM} \geq 1\right) \tag{18}$$

$$n_{transferring}(t) = int\left(k_{CTM-T2}(t) \cdot \Delta x_{CTM}\right) \tag{19}$$

$$k_{CTM-T2}(t) = k_{CTM-T2}(t) - n_{transferring}(t) \cdot \Delta x_{CTM} \tag{20}$$

$$n_{CTM-T2}(t) = n_{CTM-T2}(t) - n_{transferring}(t) \tag{21}$$

$$n_{CA\_T2}(t) = n_{CA\_T2}(t) + n_{transferring}(t) \tag{22}$$

With regard to the example shown in Fig. 17, the total number of vehicles in the transition zone at time t is equal to 1.70, obtained

Fig. 17. Transition from CTM to CA with a cumulative transition cell. The numbers in the CA cells are the speeds of the vehicles, while the values on the CTM cells are the number of vehicles.

by adding one vehicle in the CA model (which has a speed of 6 cells/s) to 0.7 vehicles in the macroscopic transition cell.

In time t the density of the CTM section is such that it has 0.70 vehicles. In time t + 1 there is a flow from the incoming cell of 0.50 veh/s, increasing the number of vehicles to 1.20, so since an entire vehicle is contained in this cell, it is transferred to the CA section in the same time step t + 1 with the mentioned procedure.

The incoming flow from the CTM model to the CTM section depends on the density of the whole transition, considering the density of the CTM section and the number of vehicles in the CA component, so if the CA model is congested or if there is even a queue, then this condition arrives to the transition zone, increasing its density and lowering the flow that the CTM section can receive from the CTM model, propagating the congestion upstream.

Furthermore, in order to compare the proposed model with a benchmark model, a numerical application was run considering a link 300 m long with a signalized junction at the end. In terms of demand, to test the impact of the undersaturation and oversaturation conditions, three different entry flows were tested: the first was 400 veh/h, the second, 800 veh/h, and the third, 1200 veh/h. In Fig. 18 the layout in terms of the hybrid model is displayed, and the details of the cellular automata model and cell transmission model are shown.

Comparison among models highlights that in the case of low demand (undersaturation) all models provide very similar results. In particular, the proposed hybrid model CA&CTM is very similar to the other benchmark models with respect to both indicators of travel times and queues. However, in the case of higher demand (oversaturation), microscopic models show lower values travel times whilst the estimated values of the queues are higher than the values achieved with the other models. In particular, the proposed hybrid model behaves very similarly to the CTM and CA models. Further details regarding the numerical results are shown in Table 12 below.

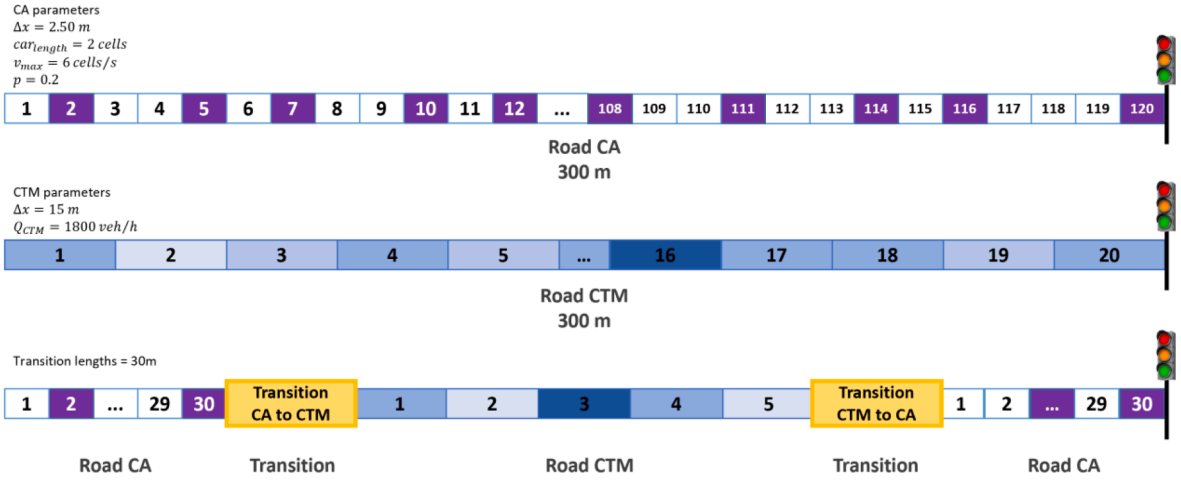

Fig. 18. Urban link layout with signalized junction.

Table 12
Numerical results of the link application.

	Travel time [veh s]	Max queue [veh]	Mean queue [veh]
Scenario Flow 1 [400 veh/h]			
CA	453.3	5.9	1.7
CTM	449.4	5.9	1.7
CA&CTM	***450.1***	***5.9***	***1.7***
Scenario Flow 1 [800 veh/h]			
CA	1023.5	11.9	4.1
CTM	1013.7	12.0	3.4
CA&CTM	***1022.4***	***12.0***	***4.3***
Scenario Flow 1 [1200 veh/h]			
CA	15585.7	44.5	38.3
CTM	15032.9	32.2	13.1
CA&CTM	***16357.4***	***34.5***	***26.1***

Appendix B

B.1. Trajectory extraction tool for traffic control systems applications (TET-TCSA)

The tool has been developed to extract, from a large trajectory dataset, portions of vehicle trajectory which drive through a selected network area.

This choice allows the development of a flexible tool useful also for applications in the urban environment for interacting intersections (Cantarella et al., 2015; Di Pace, 2020; Memoli et al., 2017).

In this work, the tool is applied to extract portions of individual trajectories in the nearby of two traffic control systems (500 m before and after each intersection). The tool is developed in MATLAB R2019b environment to be easily integrated with other models/software.

In particular, TET-TCSA takes as input data input data: (i) trajectories GPS and power data (timestamp, latitude, longitude, voltage and current) and (ii) control systems location (lat, lon), and provide as output (i) portion of trajectories in a specific range of the control systems (e.g., +/− 500 m) and (ii) descriptive statistics on trajectories that allows for clustering drivers' behaviors (e.g., seasonal, weekly, hourly).

In Fig. 19 and Fig. 20 an example of extracted trajectories at two consecutives signalized intersection, are reported.

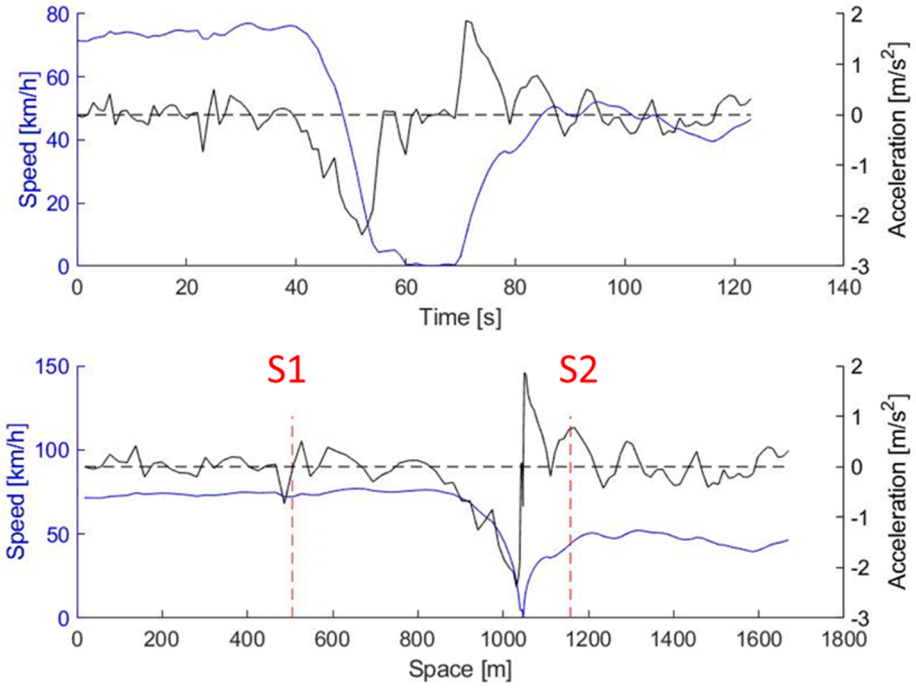

Fig. 19. Example of extracted trajectory involving 2 control systems. [Black Line is the acceleration, blue line is the speed, dot red lines represent the first-upstream (S1) and second-downstream (S2) traffic control systems.] (For interpretation of the references to colour in this figure legend, the reader is referred to the web version of this article.)

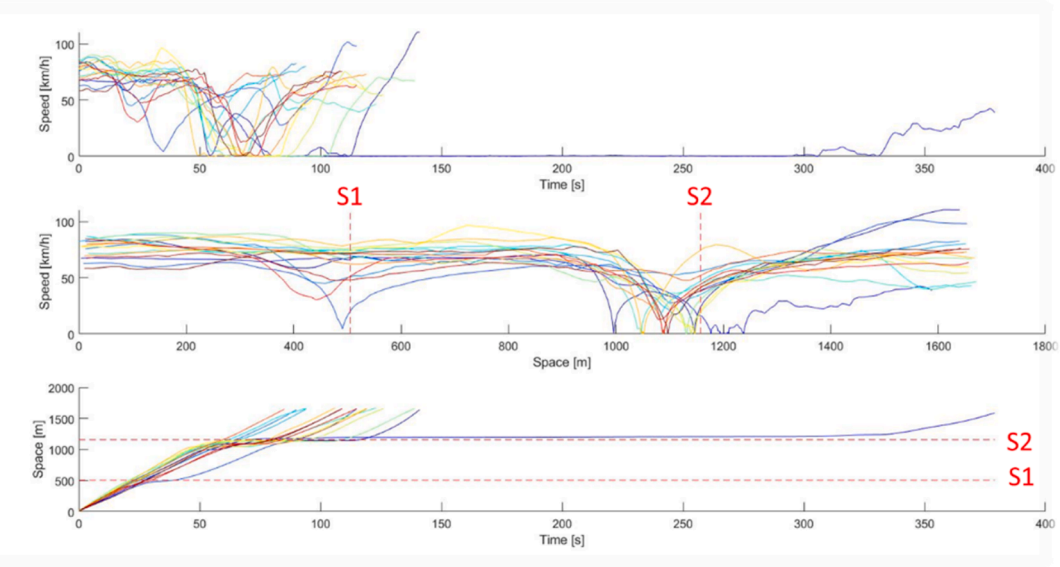

Fig. 20. Example of 12 extracted trajectories, on the same path, involving 2 consecutive control systems. The dot red lines represent the first (S1) and second (S2) traffic control systems. (For interpretation of the references to colour in this figure legend, the reader is referred to the web version of this article.)

B.2. VT-CPEM calibration with extracted real-word data at signalized intersection

In an integration with a traffic control strategy, the energy consumption is expected to enter in the objective function together with the total time spent and other measures of performance upon which control strategy is designed. To this aim, a first step is that of applying an energy consumption model to simulate EVs consumptions in proximity of the intersection. In this work, the VT-CPEM has been adopted. In particular, the model parameters are calibrated against the trajectory data extracted using the TET-TCSA.

B.2.1 Dataset statistics

The dataset is composed of 12 trajectories collected from the CAN bus of the EV tested. These data included the instantaneous power required for traction and for this reason has been possible proceed with the calibration with the output of the VT-CPEM. A summary statics of the kinematics paraments and energy consumption/recovered of the dataset is reported in Table 13.

Table 13
Summary statistics for the trajectories' dataset adopted for the calibration.

Distance [km]	Mean	1,284
	Std dvn	*0,021*
Duration [s]	Mean	77,583
	Std dvn	*20,118*
Average speed [km/h]	Mean	62,152
	Std dvn	13,465
Maximum speed [km/h]	Mean	82,743
	Std dvn	*8,905*
Max acceleration [m/s^2]	Mean	1,146
	Std dvn	*0,609*
Max deceleration [m/s^2]	Mean	−2,188
	Std dvn	*1,029*
Average slope [%]	Mean	0,002
	Std dvn	*0,003*
Energy consumption [kWh/(veh * km)]	Mean	0,096
	Std dvn	*0,020*
Energy recovered [kWh/(veh * km)]	Mean	−0,053
	Std dvn	*0,017*

B.2.2 Calibration setup and results

The dataset was processed to allow the calibration of the VT-CPEM for including the energy consumption in a traffic control systems strategy for EVs, by adopting as objective function a goodness-of-fit measure contrasting the total observed traction power P_T for each second on each trip with the corresponding model estimate given by equations (8). That is, by definition, P_T is expressed in [kW].

Four parameters are calibrated: the three efficiency parameters ($\eta_{BAT}, \eta_{DL}, \eta_{EM}$) and the parameter α entering in the regenerative braking energy efficiency (η_{RB}) via equation (9).

The objective function to minimize for the estimation of parameters is the sum of root mean square errors between observed and modelled traction power P_T in each second of the trip and for each trip.

$$\mathrm{F}(\boldsymbol{\beta}) = \sum\nolimits_{trip=1}^{N_{trips}} \sqrt{\frac{\sum_{i=1}^{T_{trip}} \left[P_{T_{trip}}^{sim}(i,\boldsymbol{\beta}) - P_{T_{trip}}^{obs}(i) \right]^2}{T_{trip}}} \tag{23}$$

Extracted trajectory data refers to the same vehicle. Thus, a single vector of four parameters **β** has been estimated for the full set of trips, yielding the following estimator:

$$\boldsymbol{\beta}^* = \underset{\boldsymbol{\beta} \in S_{\beta}}{\mathrm{argmin}} \mathrm{F}(\boldsymbol{\beta}) \tag{24}$$

The optimization problems (23)-(24) have been solved by means of a genetic algorithm (GA). This method turned out to have greater chance of finding the global solution of the optimization problem than gradient-based approaches in case of highly non-linear models. The GA was setup with an initial population of 1000 and a number of generations equal to 100, to increase the coverage of the domain of the parameters and a higher chance to detect the global optimum (Holland and Goldberg, 1989; Storn, 1996). Estimation times corresponding to this GA setup were however satisfactory.

In terms of optimization domain, upper/lower bounds for the parameters to estimate were set as illustrated in Table 14. Specifically, upper and lower bounds for the three efficiency parameters ($\eta_{BAT}, \eta_{DL}, \eta_{EM}$) have been identified according to the relevant literature (Hayes et al., 2011; Helms et al., 2010; Tie and Tan, 2013; Waide and Brunner, 2011), whilst the parameter α in the equation (9) for regenerative braking energy efficiency (η_{RB}) was constrained in the [0.005–1] range reported previously.

Table 15 reports the results of the parameter calibration of the VT-CPEM following the approach previously described in this section.

Moreover, the percentage error (PE) between the total simulated and observed energy consumption and recovery is reported in Table 16.

Results show that the PE is about the 2 %.

Table 14
Upper and lower bounds of parameters to estimate.

	η_{EM}	α	η_{BATT}	η_{DL}
Lower bound	0.90	0.005	0.90	0.90
Upper bound	0.98	1	0.98	0.98

Table 15
Calibrated parameters: values identified.

η_{EM}	α	η_{BATT}	η_{DL}
0.979	0.079	0.955	0.969

Table 16
Impact on the energy consumption and recovery.

		Observed	Simulated	PE [%]
Energy consumption [kWh/(veh * km)]	Mean	0.096	0.094	−2.1 %
Energy recovered [kWh/(veh * km)]	Mean	−0.053	−0.052	−1.9 %

Appendix C

C.1. Speed optimization/traffic lights control and speed optimization (GLOSA)

The considered speed optimization strategy has been applied in a bi-level optimization framework by combining the mono-criterion optimization based on the TTS minimization at the first level with the speed optimization aiming at the fuel consumption minimization at the second level (i.e., the Traffic lights control and Speed Optimization, GLOSA). The solution algorithm is based on an iterative procedure aiming at the best performing sub-optimal solutions able to satisfy both criteria.

In terms of speed optimization, the main purpose of the approach adopted in this paper is to ensure the arrival of the vehicles during the green light stages avoiding any stopping stage then the variations speed of a vehicle approaching to the intersection make it possible to reduce the fuel consumption based on the signal timing. In the following the details about the variables definition and the model formulation are displayed.

C.1.1. Variables' definitions

Let:

- $cell_{length}$ be the length of each cell in the Cellular Automata model, microscopic section of the Hybrid Traffic Flow model, equal to 2.5 m.
- v_{max} be the free flow desired speed, parameter of the Cellular Automata model, which can either be equal to:
  - o $base_{speed}$ the base speed value for the non-connected vehicles, equal to 6 cells/s (15 m/s)
  - o $base_{speed\text{-}CAV}$ be base speed value for the connected vehicles, in cells/s, optimized and which verifies:
    - $max_{speed\text{-}CAV}$ be the upper limit of the desired speed for the connected vehicles on the Cellular Automata model, in cells/s.
    - $min_{speed\text{-}CAV}$ be the lower limit of the desired speed for the connected vehicles on the Cellular Automata model, in cells/s.
- $optimization_{distance}$ be the distance upstream to the intersection along which the speed of the connected vehicles is optimized, set to 200 m.
- $green_{\_time}$ be the length of the green splits of the current approach/link
- last_cell be the cell index at the end of the current approach/link
- $distance_{to\_traffic\_light}$ be the distance between the current position of the vehicle to the intersection downstream of the current approach/link, in cells.
- $time_{with\_desired\_speed}$ be the number of time steps that the current vehicle would require to arrive to the intersection with the base desired speed ($base_{speed\text{-}CAV}$).
- $stage_{when\_arriving}$ be the stage of the traffic light at the time step of the vehicles' estimated arrival to the intersection
- $cycle_{length}$ be the length of the cycle, common to all intersections, set to 90 s.
- $count_{accelerated}$ be the number of connected vehicles that are travelling at a faster speed than the base, in the current link and time step.
- active_stage($time_{step}$) be the active stage of the traffic light at the considered time step
- $slower_{delta\_time}$ the number of time steps, larger than $time_{with\_desired\_speed}$, for the connected vehicle to arrive at the intersection with the next green light for the current approach. With its value and the distance to the intersection, the $slower_{speed}$ is calculated.
- $faster_{delta\_time}$ the number of time steps, lower than $time_{with\_desired\_speed}$, for the connected vehicle to arrive at the intersection with the green light at the previous cycle of the $slower_{delta\_time}$. With its value and the distance to the intersection, the $faster_{speed}$ is calculated.

C.1.2. Model formulation

The microscopic section before an intersection is modelled with a Cellular Automata model, which consists of four rules applied at each time step, and for each vehicle on the road. One of the parameters of this model is the desired speed (v_{max}) of the vehicles, set to 6 cells/s (equal to 15 m/s). This value is fixed for the non-connected vehicles, but variable for the connected vehicles when they are close to the intersection, depending on the status of the traffic light when the vehicle is estimated to arrive. This parameter is optimized before applying the Cellular Automata model.

For each connected vehicle located 200 m before the intersection, first the estimated number of time steps ($time_{with\_desired\_speed}$) for the vehicle to arrive to the intersection is calculated considering the distance to it ($distance_{to\_traffic\_light}$), and the base desired speed ($base_{speed}$). If the traffic light is green at such time step, the desired speed of the vehicle is not modified. However, if the traffic light is red, then the $slower_{delta\_time}$ is calculated, using the $time_{with\_desired\_speed}$ as a base, until the traffic light is green for the current approach. Then, the $faster_{delta\_time}$ is calculated, considering the value of the $slower_{delta\_time}$, the cycle length, the duration of the green light for the current approach, and the number connected vehicles which were already set with a desired speed greater than the base value on the current approach.

After obtaining the slower and the faster delta times, the distance of the vehicle to the intersection is divided by those values to obtain the slower speed and the faster speed with respect to the base desired speed. These values are rounded to the previous integer for the slower speed, and the next integer for the faster speed, since the variable speed in the Cellular Automata model is expressed in

terms of cells/s.

After calculating the faster and slower speeds, they are verified to comply with the limits set. First, the faster speed is verified to be lower or equal to the upper limit $max_{speed\text{-}CAV}$, and >1, to avoid negative delta times. If such conditions are met, the desired speed (v_{max}) for the current vehicle is set to the calculated faster speed, and the procedure continues with the cellular automata model. However, if such conditions are not met, then the slower speed is verified to be greater or equal to the lower limit $min_{speed\text{-}CAV}$ and the desired speed (v_{max}) is set to the value of the slower speed. If neither of the conditions are met, then the desired speed (v_{max}) is set with the base value for the connected vehicles ($base_{speed\text{-}CAV}$).

Then, with the set v_{max}, the Cellular Automata procedure continues applying its four rules. At each time step, and for each vehicle *i* on the road, their current speed $v_i(t)$ and position $x_i(t)$ are updated as:

Slowing down Obtain the *gap* at time t. If **speed** > *gap*, then slow down.

Acceleration If **speed** < *gap* and **speed** < v_{max}, then accelerate by one.

$$v_i^*(t+1) = \min(v_i(t)+1, v_0, g_i) \tag{25}$$

Randomization

(Dawdling rule) If **speed** > 0, then with probability *p* (dawdling probability, that is the random term) reduce it by one.

$$v_i(t+1) = \begin{cases} max(v_i^*(t+1)-1) & \frac{with\ probability\ p}{otherwise} \\ v_i^*(t+1) \end{cases} \tag{26}$$

Car motion Update the position.

$$x_i(t+1) = x_i(t) + v_i(t+1) \tag{27}$$

The proposed speed optimization has been applied in a bi-level optimization framework by combining the mono-criterion optimization based on the TTS minimization at the first level with the speed optimization aiming at the fuel consumption minimization at the second level. AS already explained at the beginning pf the section, the solution algorithm is based on an iterative procedure aiming at the best performing sub-optimal solutions able to satisfy both criteria.

References

Al Islam, S.B., Hajbabaie, A., 2017. Distributed coordinated signal timing optimization in connected transportation networks. Transport. Res. Part C: Emerg. Technol. 80, 272–285.

Ali, M.M., Törn, A., 2004. Population set-based global optimization algorithms: some modifications and numerical studies. Comput. Oper. Res. 31, 1703–1725.

Arcidiacono, V., Maineri, L., Tsiakmakis, S., Fontaras, G., Thiel, C., Ciuffo, B., 2017. fUel-SAVing trip plannEr (U-SAVE): a product of the JRC PoC Instrument.

Asadi, B., Vahidi, A., 2010. Predictive cruise control: utilizing upcoming traffic signal information for improving fuel economy and reducing trip time. IEEE Trans. Control Syst. Technol. 19 (3), 707–714.

Bandeira, J.M., Fernandes, P., Fontes, T., Pereira, S.R., Khattak, A.J., Coelho, M.C., 2018. Exploring multiple eco-routing guidance strategies in a commuting corridor. Int. J. Sustain. Transport. 12 (1), 53–65.

Beak, B., Head, K.L., Feng, Y., 2017. Adaptive coordination based on connected vehicle technology. Transp. Res. Rec. 2619 (1), 1–12.

Brooker, A., Gonder, J., Wang, L., Wood, E., Lopp, S., Ramroth, L., 2015. FASTSim: a model to estimate vehicle efficiency, cost and performance. SAE Technical Paper.

Cantarella, G.E., de Luca, S., Di Pace, R., Memoli, S., 2015. Network Signal Setting Design: meta-heuristic optimization methods. Transp. Res. Part C Emerg. Technol. 55, 24–45.

Ciuffo, B., Fontaras, G., 2017. Models and scientific tools for regulatory purposes: the case of CO2 emissions from light duty vehicles in Europe. Energy Policy 109, 76–81.

CO2MPAS: Vehicle simulator predicting NEDC CO2 emissions from WLTP — CO2MPAS 1.6.1.post0 documentation [WWW Document], 2018. Available from: https://co2mpas.io/.

Daganzo, C.F., 1994. The cell transmission model: a dynamic representation of highway traffic consistent with the hydrodynamic theory. Transport. Res. Part B: Methodol. 28 (4), 269–287.

Das, S., Konar, A., Chakraborty, U.K., 2005. Two improved differential evolution schemes for faster global search. In: ACM-SIGEVO Proceedings of GECCO' 05, Washington D.C., pp. 991–998.

De Nunzio, G., De Wit, C.C., Moulin, P., Di Domenico, D., 2016. Eco-driving in urban traffic networks using traffic signals information. Int. J. Robust Nonlinear Control 26 (6), 1307–1324.

Di Pace, R., 2020. A traffic control framework for urban networks based on within-day dynamic traffic flow models. Transportmetrica A: Transport Science 16, 234–269.

Fajardo, D., Au, T.C., Waller, S.T., Stone, P., Yang, D., 2011. Automated intersection control: performance of future innovation versus current traffic signal control. Transp. Res. Rec. 2259 (1), 223–232.

Feng, Y., Head, K.L., Khoshmagham, S., Zamanipour, M., 2015. A real-time adaptive signal control in a connected vehicle environment. Transport. Res. Part C: Emerg. Technol. 55, 460–473.

Feng, Y., Zamanipour, M., Head, K.L., Khoshmagham, S., 2016. Connected vehicle–based adaptive signal control and applications. Transp. Res. Rec. 2558 (1), 11–19.

Fiori, C., Ahn, K., Rakha, H.A., 2016. Power-based electric vehicle energy consumption model: model development and validation. Appl. Energy 168, 257–268.

Fiori, C., Ahn, K., Rakha, H.A., 2018. Microscopic series plug-in hybrid electric vehicle energy consumption model: model development and validation. Transp. Res. Part Transp. Environ. 63, 175–185.

Fiori, C., Arcidiacono, V., Fontaras, G., Makridis, M., Mattas, K., Marzano, V., Thiel, C., Ciuffo, B., 2019. The effect of electrified mobility on the relationship between traffic conditions and energy consumption. Transp. Res. Part Transp. Environ. 67, 275–290.

Fiori, C., Marzano, V., 2018. Modelling energy consumption of electric freight vehicles in urban pickup/delivery operations: analysis and estimation on a real-world dataset. Transp. Res. Part Transp. Environ. 65, 658–673.
Fiori, C., Marzano, V., Punzo, V., Montanino, M., 2020. Energy consumption modeling in presence of uncertainty. IEEE Trans. Intell. Transp. Syst.
Girianna, M., Benekohal, R.F., 2004. Using genetic algorithms to design signal coordination for oversaturated networks. J. Intell. Transport. Syst. 8 (2), 117–129.
Goodall, N.J., Smith, B.L., Park, B., 2013. Traffic signal control with connected vehicles. Transp. Res. Rec. 2381 (1), 65–72.
Han, Y., Wang, M., He, Z., Li, Z., Wang, H., Liu, P., 2021. A linear Lagrangian model predictive controller of macro-and micro-variable speed limits to eliminate freeway jam waves. Transport. Res. Part C: Emerg. Technol. 128, 103121.
Hayes, J.G., De Oliveira, R.P.R., Vaughan, S., Egan, M.G., 2011. Simplified electric vehicle power train models and range estimation. In: 2011 IEEE Vehicle Power and Propulsion Conference (VPPC). IEEE, pp. 1–5.
He, X., Liu, H.X., Liu, X., 2015. Optimal vehicle speed trajectory on a signalized arterial with consideration of queue. Transport. Res. Part C: Emerg. Technol. 61, 106–120.
Helms, H., Pehnt, M., Lambrecht, U., Liebich, A., 2010. Electric vehicle and plug-in hybrid energy efficiency and life cycle emissions. In: 18th International Symposium Transport and Air Pollution. Citeseer, pp. 113–124.
Holland, J.H., Goldberg, D., 1989. Genetic Algorithms in Search, Optimization and Machine Learning. Addison-Wesley, Boston, MA.
Homchaudhuri, B., Vahidi, A., Pisu, P., 2017. Fast model predictive control-based fuel efficient control strategy for a group of connected vehicles in urban road conditions. IEEE Trans. Control Syst. Technol. 25 (2), 760–767. https://doi.org/10.1109/tcst.2016.2572603.
Jiang, Y., Wang, S., Yao, Z., Zhao, B., & Wang, Y. (2021). A cellular automata model for mixed traffic flow considering the driving behavior of connected automated vehicle platoons. Physica A: Statistical Mechanics and its Applications, 582, 126262.
Kamalanathsharma, R.K., Rakha, H.A., Yang, H., 2015. Networkwide impacts of vehicle ecospeed control in the vicinity of traffic signalized intersections. Transp. Res. Rec. 2503, 91–99.
Katsaros, K., Kernchen, R., Dianati, M., Rieck, D., (2011, July). Performance study of a Green Light Optimized Speed Advisory (GLOSA) application using an integrated cooperative ITS simulation platform. In: 2011 7th International Wireless Communications and Mobile Computing Conference. IEEE, pp. 918–923.
Kim, N., Rousseau, A., Rask, E., 2012. Autonomie model validation with test data for 2010 Toyota Prius. SAE Technical Paper.
Koski, J., Silvennoinen, R., 1987. Norm methods and partial weighting in multicriterion optimization of structures. Int. J. Numer. Meth. Eng. 24, 1101–1121.
Koski, J., 1981. Multicriterion Optimization in Structural Design. Tampere Univ of Technology (Finland).
Lampinen, J., Storn, R., 2004. Differential evolution. In: New Optimization Techniques in Engineering. Springer, pp. 123–166.
Lee, B., Lee, S., Cherry, J., Neam, A., Sanchez, J., Nam, E., 2013. Development of advanced light-duty powertrain and hybrid analysis tool. SAE Technical Paper.
Levin, M.W., Boyles, S.D., 2016a. A cell transmission model for dynamic lane reversal with autonomous vehicles. Transport. Res. Part C: Emerg. Technol. 68, 126–143.
Levin, M.W., Boyles, S.D., 2016b. A multiclass cell transmission model for shared human and autonomous vehicle roads. Transport. Res. Part C: Emerg. Technol. 62, 103–116.
Li, W., Ban, X., 2018. Connected vehicles based traffic signal timing optimization. IEEE Trans. Intell. Transp. Syst. 20 (12), 4354–4366.
Li, M., Wu, X., He, X., Yu, G., Wang, Y., 2018. An eco-driving system for electric vehicles with signal control under V2X environment. Transp. Res. Part C Emerg. Technol. 93, 335–350.
Liebner, M., Klanner, F., Baumann, M., Ruhhammer, C., Stiller, C., 2013. Velocity-based driver intent inference at urban intersections in the presence of preceding vehicles. IEEE Intell. Transp. Syst. Mag. 5 (2), 10–21.
Liu, K., Liu, D., Li, C., Yamamoto, T., 2019. Eco-speed guidance for the mixed traffic of electric vehicles and internal combustion engine vehicles at an isolated signalized intersection. Sustainability 11, 5636.
Liu, M., Zhao, J., Hoogendoorn, S., Wang, M., 2022. A single-layer approach for joint optimization of traffic signals and cooperative vehicle trajectories at isolated intersections. Transport. Res. Part C: Emerg. Technol. 134, 103459.
Luo, Y., Li, S., Zhang, S., Qin, Z., Li, K., 2017. Green light optimal speed advisory for hybrid electric vehicles. Mech. Syst. Signal Process. 87, 30–44.
Ma, J., Li, X., Zhou, F., Hu, J., Park, B.B., 2017. Parsimonious shooting heuristic for trajectory design of connected automated traffic part II: computational issues and optimization. Transport. Res. Part B: Methodol. 95, 421–441.
Marmaras, C., Xydas, E., Cipcigan, L., 2017. Simulation of electric vehicle driver behaviour in road transport and electric power networks. Transp. Res. Part C Emerg. Technol. 80, 239–256.
Memoli, S., Cantarella, G.E., de Luca, S., Di Pace, R., 2017. Network signal setting design with stage sequence optimization. Transp. Res. Part B Methodol. 100, 20–42.
Mogno, C., Fontaras, G., Arcidiacono, V., Komnos, D., Pavlovic, J., Ciuffo, B., Valverde, V., 2020. The application of the CO2MPAS model for vehicle CO2 emissions estimation over real traffic conditions. Transp. Policy.
Nagel, K., Schreckenberg, M., 1992. A cellular automaton model for freeway traffic. J. Phys. I 2 (12), 2221–2229.
Newman, K.A., Doorlag, M., Barba, D., 2016. Modeling of a conventional mid-size car with CVT using ALPHA and comparable powertrain technologies. SAE Technical Paper.
O'Hora, B., Perera, J., Brabazon, A., 2006. Designing radial basis function networks for classification using differential evolution. In: The 2006 IEEE International Joint Conference on Neural Network Proceedings. IEEE, pp. 2932–2937.
Park, S., Rakha, H., Ahn, K., Moran, K., 2013. Virginia Tech comprehensive power-based fuel consumption model (VT-CPFM): model validation and calibration considerations. Int. J. Transp. Sci. Technol. 2, 317–336.
Pavlovic, J., Marotta, A., Ciuffo, B., 2016. CO2 emissions and energy demands of vehicles tested under the NEDC and the new WLTP type approval test procedures. Appl. Energy 177, 661–670.
Price, K.V., 2013. Differential evolution. In: Handbook of Optimization. Springer, pp. 187–214.
Priemer, C., Friedrich, B., 2009, October. A decentralized adaptive traffic signal control using V2I communication data. In: 2009 12th International IEEE Conference on Intelligent Transportation Systems. IEEE, pp. 1–6.
Pan, T., Lam, W.H., Sumalee, A., Zhong, R., 2021. Multiclass multilane model for freeway traffic mixed with connected automated vehicles and regular human-piloted vehicles. Transportmetrica A: transport science, 17(1), 5-33.
Rakha, H.A., Ahn, K., Moran, K., Saerens, B., Van den Bulck, E., 2011. Virginia tech comprehensive power-based fuel consumption model: model development and testing. Transp. Res. Part Transp. Environ. 16, 492–503.
Rao, S.S., Freiheit, T.I., 1991. A modified game theory approach to multiobjective optimization.
Robertson, D.I., 1979. Traffic models and optimum strategies of control: a review. In: Paper for the International Symposium on Traffic Control Systems, University of California, Berkeley, August 1979. Transport and Road Research Laboratory.
Sobol, I.M., 1976. Uniformly distributed sequences with an additional uniform property. USSR Comput. Math. Math. Phys. 16, 236–242.
Stevanovic, A., Stevanovic, J., Zhang, K., Batterman, S., 2009. Optimizing traffic control to reduce fuel consumption and vehicular emissions: Integrated approach with VISSIM, CMEM, and VISGAOST. Transp. Res. Rec. J. Transp. Res. Board 105–113.
Storani, F., Di Pace, R., Bruno, F., Fiori, C., 2021. Analysis and comparison of traffic flow models: a new hybrid traffic flow model vs benchmark models. Eur. Transp. Res. Rev. 13 (1), 1–16.
Storani, F., Di Pace, R., De Luca, S., 2022a. A hybrid traffic flow model for traffic management with human-driven and connected vehicles. Transportmet. B: Transp. Dyn. 1–33.
Storani, F., Di Pace, R., De Schutter, B., 2022b. A traffic responsive control framework for signalized junctions based on hybrid traffic flow representation. J. Intell. Transport. Syst. 1–20.
Storn, R., Price, K., 1997. Differential evolution–a simple and efficient heuristic for global optimization over continuous spaces. J. Glob. Optim. 11, 341–359.
Storn, R., 1996. On the usage of differential evolution for function optimization. In: Fuzzy Information Processing Society, 1996. NAFIPS, 1996 Biennial Conference of the North American. IEEE, pp. 519–523.
Tie, S.F., Tan, C.W., 2013. A review of energy sources and energy management system in electric vehicles. Renew. Sustain. Energy Rev. 20, 82–102.

Tsiakmakis, S., Fontaras, G., Ciuffo, B., Samaras, Z., 2017. A simulation-based methodology for quantifying European passenger car fleet CO2 emissions. Appl. Energy 199, 447–465.
Waide, P., Brunner, C.U., 2011. Energy-efficiency policy opportunities for electric motor-driven systems.
Wang, M., Hoogendoorn, S.P., Daamen, W., van Arem, B., Happee, R., 2015. Game theoretic approach for predictive lane-changing and car-following control. Transport. Res. Part C: Emerg. Technol. 58, 73–92.
Wang, M., Daamen, W., Hoogendoorn, S.P., van Arem, B., 2016. Connected variable speed limits control and car-following control with vehicle-infrastructure communication to resolve stop-and-go waves. J. Intell. Transport. Syst. 20 (6), 559–572.
Wipke, K.B., Cuddy, M.R., Burch, S.D., 1999. ADVISOR 2.1: a user-friendly advanced powertrain simulation using a combined backward/forward approach. IEEE Trans. Veh. Technol. 48, 1751–1761.
Wu, X., Freese, D., Cabrera, A., Kitch, W.A., 2015a. Electric vehicles' energy consumption measurement and estimation. Transp. Res. Part Transp. Environ. 34, 52–67.
Wu, X., He, X., Yu, G., Harmandayan, A., Wang, Y., 2015b. Energy-optimal speed control for electric vehicles on signalized arterials. IEEE Trans. Intell. Transp. Syst. 16, 2786–2796.
Yang, R.J., Tseng, L., Nagy, L., Cheng, J., 1994. Feasibility study of crash optimization. ASME 549–556.
Zegeye, S.K., De Schutter, B., Hellendoorn, H., Breunesse, E., 2009. Reduction of travel times and traffic emissions using model predictive control. In: 2009 American Control Conference. IEEE, pp. 5392–5397.
Zegeye, S.K., De Schutter, B., Hellendoorn, J., Breunesse, E.A., Hegyi, A., 2013. Integrated macroscopic traffic flow, emission, and fuel consumption model for control purposes. Transp. Res. Part C Emerg. Technol. 31, 158–171.
Zhang, R., Yao, E., 2015. Eco-driving at signalised intersections for electric vehicles. IET Intell. Transp. Syst. 9, 488–497.
Zhao, J., Li, W., Wang, J., Ban, X., 2015. Dynamic traffic signal timing optimization strategy incorporating various vehicle fuel consumption characteristics. IEEE Trans. Veh. Technol. 65 (6), 3874–3887.
Zhao, H.X., He, R.C., Yin, N., 2021. Modeling of vehicle CO 2 emissions and signal timing analysis at a signalized intersection considering fuel vehicles and electric vehicles. Eur. Transp. Res. Rev.ew 13 (1), 1–15.
Zhou, F., Li, X., Ma, J., 2017. Parsimonious shooting heuristic for trajectory design of connected automated traffic part I: theoretical analysis with generalized time geography. Transport. Res. Part B: Methodol. 95, 394–420.
Zhu, F., Ukkusuri, S.V., 2017. Efficient and fair system states in dynamic transportation networks. Transport. Res. Part B: Methodol. 104, 272–289.
Zhu, F., Ukkusuri, S.V., 2018. Modeling the proactive driving behavior of connected vehicles: a cell-based simulation approach. Comput.-Aided Civ. Infrastruct. Eng. 33 (4), 262–281.
Zhu, F., Lo, H.K., Lin, H.-Z., 2013. Delay and emissions modelling for signalised intersections. Transp. B Transp. Dyn. 1, 111–135.